Toxicology 521 (2026) 154393

Contents lists available at ScienceDirect

Toxicology

journal homepage: www.elsevier.com/locate/toxicol

Bisphenol TMC exhibits greater estrogenic activity than Bisphenol A and three other structural analogues exemplified by higher estrogen receptor α-mediated gene expression and breast cancer cell proliferation

Friedrich L. Joos [a,c], Rianne E. van Diest [b,c], Martin Smieško [b,c], Marie-Christin Jäger [a,c], Manuel Kley [a,c], Alex Odermatt [a,c], Jamal Bouitbir [a,c,*]

[a] Division of Molecular and Systems Toxicology, Department of Pharmaceutical Sciences, University of Basel, Klingelbergstrasse 50, Basel 4056, Switzerland
[b] Computational Pharmacy, Department of Pharmaceutical Sciences, University of Basel, Klingelbergstrasse 50, Basel 4056, Switzerland
[c] Swiss Centre for Applied Human Toxicology (SCAHT), University of Basel, Missionsstrasse 64, , Basel 4055, Switzerland

ARTICLE INFO

Keywords:
Bisphenol A
Bisphenol TMC
Endocrine disruptor
Estrogen receptor α
Regrettable substitution
Breast cancer

ABSTRACT

Bisphenol A (BPA) and its structural analogues are widely used in plastics production, raising concern due to endocrine-disrupting properties. While many analogues share structural similarities with BPA, their endocrine-disrupting effects remain insufficiently characterized. Cyclo-di-bisphenol A diglycidyl ether (cyclo-di-BADGE), tetrabromobisphenol S (TBBPS), bisphenol SIP (BPSIP), and bisphenol TMC (BPTMC) are particularly understudied. We assessed the estrogenic activity of these four BPA analogues compared to BPA. Transactivation assays in HEK-293 cells expressing estrogen receptor alpha (ERα) revealed that BPTMC was a more potent ERα agonist than BPA, with an EC_{50} of 87 ± 20 nM *versus* 400 ± 100 nM for BPA, while the other tested analogues showed no significant agonistic activity. *In silico* analysis attributed this higher affinity to greater hydrophobicity and a bulkier bridging group between its phenolic rings. None of the compounds inhibited 17β-hydroxysteroid dehydrogenase type 1 (17β-HSD1) activity. However, BPTMC selectively inhibited 17β-HSD2 (IC_{50} = 4.8 ± 0.6 μM) but not BPA. Importantly, 24 h exposure of ERα-positive MCF-7 breast cancer cells to 1 μM BPTMC upregulated the expression of the ERα target genes *GREB1*, *TFF1*, and *PGR*, comparable to 10 nM E2, which was abolished by 100 nM of the ERα antagonist fulvestrant. Moreover, BPTMC stimulated MCF-7 cell proliferation at nanomolar concentrations over 72 h, and cell count analyses confirmed this effect. BPA also increased cell numbers, and both effects were reversed by fulvestrant. Collectively, we identified BPTMC as a potent ERα agonist capable of eliciting transcriptional and mitogenic responses at low concentrations, raising concerns about its endocrine-disrupting and breast cancer-promoting effects.

Abbreviations: ΔG_{bind}, Binding free energy; $\Delta G_{desolvation}$, Desolvation energy; 17β-HSD1, 17β-hydroxysteroid dehydrogenase type 1; 17β-HSD2, 17β-hydroxysteroid dehydrogenase type 2; ANOVA, Analysis of variance; BADGE, Bisphenol A diglycidyl ether; BPA, Bisphenol A; BPAF, Bisphenol AF; BPB, Bisphenol B; BPF, Bisphenol F; BPP, Bisphenol P; BPS, Bisphenol S; BPSIP, Bisphenol SIP; BPTMC, Bisphenol TMC; BPZ, Bisphenol Z; CSO, S-hydroxycysteine; Cyclo-di-BADGE, Cyclo-di-bisphenol A diglycidyl ether; DMEM, Dulbecco's Modified Eagle Medium; DPM, Diphenylmethane; DPP, Diphenylpropane; E1, Estrone; E2, 17β-estradiol; EC_{50}, Half-maximal effective concentration; ECHA, European Chemicals Agency; EDCs, Endocrine-disrupting chemicals; ERα, Estrogen receptor alpha; ERβ, Estrogen receptor beta; ERE, Estrogen response element; *GREB1*, Growth regulation by estrogen in breast cancer 1; HEK-293, Human embryonic kidney cells; IC_{50}, Half-maximal inhibitory concentration; LBP, Ligand-binding pocket; LogP, Lipophilicity; LogS, Solubility; MD, Molecular dynamics; MPP, Methylpiperidino pyrazole; NDGA, Nordihydroguaiaretic acid; PBTK, Physiologically-based toxicokinetic; PCOS, Polycystic ovary syndrome; *PGR*, Progesterone receptor; RMSF, Root mean square fluctuation; TBBPA, Tetrabromobisphenol A; TBBPS, Tetrabromobisphenol S; TCBPA, Tetrachlorobisphenol A; *TFF1*, Trefoil factor 1 also known as *pS2*; TMBPA, Tetramethylbisphenol A; TMBPF, Tetramethylbisphenol F.

* Correspondence to: Division of Molecular and Systems Toxicology, Department of Pharmaceutical Sciences, University of Basel, Mattenstrasse 22, Basel 4058, Switzerland.

E-mail address: jamal.bouitbir@unibas.ch (J. Bouitbir).

https://doi.org/10.1016/j.tox.2025.154393
Received 26 September 2025; Received in revised form 12 December 2025; Accepted 31 December 2025
Available online 31 December 2025

1. Introduction

Endocrine-disrupting chemicals (EDCs) are a diverse group of exogenous compounds capable of interfering with hormonal systems, potentially leading to a range of adverse health effects in humans (Diamanti-Kandarakis et al. 2009). These chemicals can mimic or antagonize natural hormones, disrupt the synthesis, protein binding, transport, and metabolism of endogenous hormones, and alter the normal functioning of hormonal pathways (Hassan et al. 2024; Schug et al. 2011).

Among the most extensively studied EDCs is bisphenol A (BPA), a synthetic monomer widely used in the production of polycarbonate plastics and epoxy resins (Michalowicz, 2014). These materials are commonly found in consumer products such as food and beverage containers, dental sealants, medical devices, and thermal paper receipts (Hoekstra and Simoneau, 2013; Manzoor et al. 2022). The widespread use of BPA and its tendency to leach from products explain its presence in various human biological fluids, including blood, urine, and breast milk (Manzoor et al. 2022; Mercogliano and Santonicola, 2018). Notably, BPA has been detected in over 90 % of samples in the European and American population (Becker et al. 2009; Calafat et al. 2008; Mustieles et al. 2020). Increasing scientific and public concern has been directed toward the potential adverse health outcomes associated with chronic BPA exposure, including obesity, diabetes mellitus, developmental abnormalities, and hormone-sensitive cancers such as breast cancer (Cull and Winn, 2024; Duenas-Moreno et al. 2023; Rochester, 2013; Seachrist et al. 2016). In addition, rising infertility rates in developed countries prompt concerns regarding the potential impact of EDCs on female and male reproductive health (ovarian and Leydig cell steroidogenesis; follicle development, and sperm production) and fertility (Mlynarcikova et al. 2014; Odermatt et al. 2016). Hormone- and metabolism-related disorders such as polycystic ovary syndrome (PCOS) and endometriosis are increasingly recognized as susceptible to EDCs exposure (Bruni et al. 2022). Emerging evidence suggests a strong association between BPA exposure and the pathogenesis of PCOS, the most prevalent endocrine disorder among reproductive-aged women (March et al. 2010; Neuvonen et al. 2023; Srnovrsnik et al. 2023).

Several studies have demonstrated that many EDCs exert their effects by targeting estrogen receptor (ER) signaling. These chemicals can mimic or block the actions of endogenous estrogens, thereby disrupting ER-mediated transcriptional activity in both cellular and animal models (Diamanti-Kandarakis et al. 2009). Mechanistically, BPA can bind to and activate both ERα and ERβ, triggering estrogenic signaling pathways and contributing to its endocrine-disrupting properties (Stanojevic and Sollner Dolenc, 2025; Welshons et al. 2006). ERα, in particular, belongs to the nuclear receptor superfamily and can be activated by ligands like 17β-estradiol (E2), leading to its interaction with estrogen response elements (EREs) and subsequent transcription of target genes (Arnal et al. 2017). However, it can also be activated by other signaling pathways in a ligand-independent manner (Deroo and Korach, 2006).

In addition to acting via ERs, BPA also affects estrogen homeostasis by altering steroid hormone biosynthesis. One key target group includes the hydroxysteroid dehydrogenases, particularly 17β-hydroxysteroid dehydrogenase type 1 (17β-HSD1) and type 2 (17β-HSD2). 17β-HSD1 catalyzes the conversion of estrone (E1), a weak estrogen, into E2, the most potent endogenous estrogen, thereby enhancing estrogenic activity (Hilborn et al. 2017). This enzyme is expressed in various estrogen-responsive tissues, including the breast, ovary, placenta, and endometrium (Miettinen et al. 1996; Poutanen et al. 1992a; Poutanen et al. 1992b; Soderqvist et al. 1998). BPA has been reported to inhibit 17β-HSD1 with an IC_{50} of approximately 113 μM (Chen et al. 2023), a concentration unlikely to be reached in an exposure scenario *in vivo* and thus not considered to be toxicologically relevant. In contrast, 17β-HSD2 catalyzes the oxidative conversion of E2 back to E1, thus reducing estrogenic potency, and is highly expressed in tissues such as the breast, uterus, prostate, liver, and intestine (Peltoketo et al. 1999). To date, no data are available regarding the inhibition of 17β-HSD2 by BPA or its analogues, underscoring the need for further investigation.

The growing evidence for adverse health effects of BPA has led to restrictions and bans limiting its use in consumer products, *e.g.*, in Canada, Europe, and the USA beginning as early as 2008, which have been progressively extended from baby bottles to thermal paper receipts, and more recently, the complete ban in food contact materials (European_Commission, 2024; Government_of_Canada, 2023; Kiss, 2013; Sieck et al. 2024). In response, the industry has introduced a variety of structural analogues such as bisphenol SIP (BPSIP, also referred to as D-8 or Wincon-8), bisphenol TMC (BPTMC), tetrabromobisphenol S (TBBPS), and bisphenol A diglycidyl ether (BADGE) as replacements for BPA. Cyclo-di-bisphenol A diglycidyl ether (Cyclo-di-BADGE), a cyclic product formed from BPA and BADGE during the production of epoxy resins, is a known contaminant in food contact materials. These derivatives share similar chemical structures and physicochemical properties with BPA, raising concerns that they may also exhibit endocrine-disrupting potential (See chemical structures in Fig. 1). Although manufacturers promote these chemicals as safer alternatives to BPA, scientists and regulators emphasize that further research is essential to assess their safety and understand their potential long-term effects on human health.

Given the urgent need for thorough toxicological and mechanistic evaluation of BPA analogues, we aimed to investigate the potential endocrine-disrupting activities of four BPA analogues, namely cyclo-di-BADGE, TBBPS, BPSIP, and BPTMC. Specifically, we assessed their ERα agonistic and antagonistic activities, along with their ability to inhibit 17β-HSD1 and 17β-HSD2. Additionally, *in silico* analysis was employed to investigate the underlying structural basis for estrogenic activity towards ERα. These endpoints were selected to provide a comparative understanding of the hormonal activity of BPA analogues relative to BPA itself and to inform risk assessment and regulatory decisions regarding their use.

2. Materials and methods

2.1. Chemicals and reagents

BPA (CAS# 80–05–7, Cat# 239658, purity ≥ 99 %) was purchased from Merck (Darmstadt, Germany), cyclo-di-BADGE (CAS#

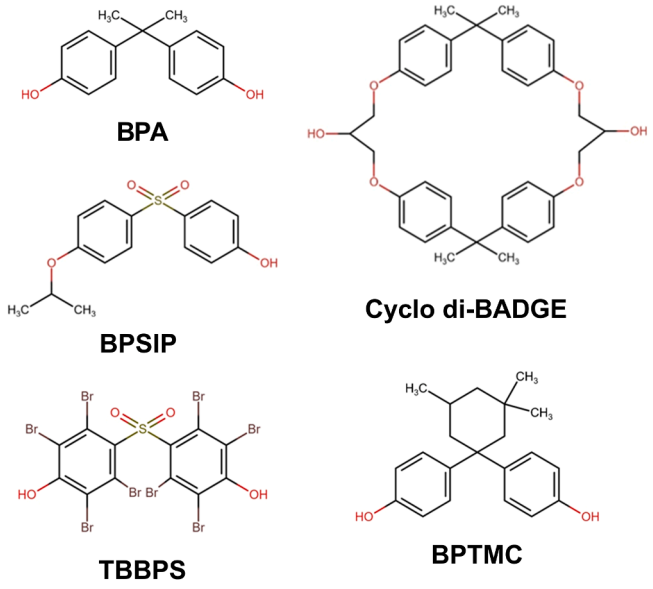

Fig. 1. Chemical structures of bisphenol A (BPA) and the four derivatives: cyclo-di-bisphenol A diglycidyl ether (cyclo-di-BADGE), tetrabromobisphenol S (TBBPS), bisphenol SIP (BPSIP), and bisphenol TMC (BPTMC).

20583–87–3, Cat# C10586.36, purity ≥ 95 %) from Chiron AS (Trondheim, Norway), TBBPS (CAS# 39635–79–5, Cat# FT147403, purity ≥ 95 %) from Biosynth AG (Staad, Switzerland), BPSIP (CAS# 95235–30–6, Cat# CBLQA-6028, purity ≥ 98 %), and BPTMC (CAS# 129188–99–4, Cat# CBLQV-5232, purity ≥ 98 %) from Chemie Brunschwig AG (Basel, Switzerland). Dimethyl sulfoxide (DMSO) was purchased from Huberlab (Aesch, Switzerland; CAS# 67–68–5, Cat# A3672). Fulvestrant (Merck; CAS# 129453–61–8, Cat# I4409) was a generous gift from Prof. Mohamed Bentires-Alj (Department of Biomedicine, University of Basel, Switzerland). Methylpiperidino pyrazole (MPP, CAS# 911295–24–4, Cat# M7068), apigenin (CAS# 520–36–5, Cat# A3145), nordihydroguaiaretic acid (NDGA, CAS# 500–38–9, Cat# 74540), E1 (CAS# 53–16–7, Cat# E9750), E2 (CAS# 50–28–2, Cat# E8875), and Triton™ X-100 (CAS# 9036–19–5, Cat# X100) were purchased from Merck. Stock solutions were prepared in DMSO and stored at −20°C.

Dulbecco's Modified Eagle Medium (DMEM, 4.5 g/L glucose, 2 mM L-glutamine), penicillin/streptomycin (10,000 U/mL and 10 mg/mL, respectively), 10 mM HEPES buffer, pH 7.4, and MEM non-essential amino acids were purchased from BioConcept (Allschwil, Switzerland). Fetal bovine serum (FBS, Cat# S1810; Batch S00CJ) was purchased from Biowest (Nuaillé, France). The Tropix kit was obtained from Applied Biosystems (Foster City, CA, USA). [6,7–3H]-estrone was purchased from Anawa (Kloten, Switzerland) and [2,4,6,7–3H]-estradiol from PerkinElmer (Boston, MA, USA), and all other chemicals from Merck if not stated otherwise. The plasmids pRC/CMV-17βHSD1 (originally from Dr. Reijo Vihko, University of Oulu, Finland) and pCMV6–17βHSD2 were kindly provided by the late Dr. Stefan Andersson (University of Texas Southwestern Medical Center, Dallas, Texas, USA) (Khan et al. 2004; Wu et al. 1993).

2.2. Cell culture

Human Embryonic Kidney cells (HEK-293, ATCC, Manassas, VA, USA) were cultured in DMEM high glucose (4.5 g/L), 2 mM L-glutamine, supplemented with 10 % FBS, 10 mM HEPES, pH 7.4, 100 μg/mL streptomycin and 100 U/mL penicillin, and 1 % (v/v) 100x MEM non-essential amino acids. MCF-7 cells (HTB-22, ATCC) were cultured in DMEM high glucose (4.5 g/L), 2 mM L-glutamine, supplemented with 10 % FBS and 10 mM HEPES, pH 7.4. Both cell lines were cultured under standard conditions (37°C, 5 % CO_2) in an incubator (Thermo Fisher Scientific, Waltham, USA). Passaging was carried out via trypsinization with 1x trypsin-EDTA (Merck; Cat# T4174; 1:10 diluted with PBS), and cell counts were determined using the Countess 3 FL automated cell counter (Thermo Fisher Scientific) with the trypan blue exclusion method.

2.3. ERα-dependent transactivation assay

HEK-293 cells (100,000 cells/well in 500 μL medium/well) were seeded in a 24-well plate (Sarstedt, Nümbrecht, Germany) coated with 0.005 % poly-L-lysine (0.01 % poly-L-lysine solution (Sigma-Aldrich, Steinheim, Germany) mixed 1:1 with PBS) and left to attach for 18 h. Plasmid DNA (390 ng/well for ERα; 25 ng/well for CMV-LacZ; 390 ng/well for 4x ERE Luc) was diluted in 37°C water to a final volume of 30 μL/well. A volume of 10 μL/well of 37°C 2 M $CaCl_2$ was added slowly. The mixture was pipetted dropwise into an equal volume of 37°C 2x BEST solution (8.0 g NaCl; 0.198 g $Na_2HPO_4 \cdot 7\ H_2O$; 5.3 g N,N-bis[2-hydroxyethyl]-2-aminoethane sulfonic acid (Sigma-Aldrich), add water to 500 mL, pH 7.0) and incubated at room temperature (RT) for 15 min. The cells were transfected by adding 80 μL of this transfection mixture to the medium of each well. After a period of 4 h, the supernatant in each well was removed and replaced with fresh medium (500 μL/well). The treatment medium was phenol-red free DMEM high glucose (4.5 g/L) (Sigma-Aldrich) supplemented with L-glutamine, 10 mM HEPES, pH 7.4 (BioConcept), 100 μg/mL streptomycin and 100 U/mL penicillin, and 1 % (v/v) 100x MEM non-essential amino acids (BioConcept) as well as 10 % charcoal-treated FBS. The charcoal treatment was performed to deprive the FBS of E2. For charcoal treatment, 50 mL FBS were mixed with 2 g of activated charcoal (Sigma-Aldrich) and shaken at 4°C overnight. The suspension was subjected to centrifugation at 4°C and 15,000 g for 10 min, after which the supernatant was decanted into a new tube. The aforementioned procedure was repeated for a total of two overnight charcoal treatments. Following the final charcoal treatment, the FBS was sterile filtered using a 0.2 μm Filtropur S 0.2 filter (Sarstedt). One h prior to the treatment, the medium was replaced with the E2-deprived medium. Subsequently, the cell supernatant was replaced with 500 μL of the same medium containing the test compounds at their respective concentrations and a fixed amount of 0.1 % DMSO. To investigate possible antagonistic effects of test compounds on ERα, 20 μL/well of 52 nM E2 was added after another hour, resulting in a total concentration of 2 nM E2 in the well. For the assessment of agonistic and antagonistic effects of BPA and the four analogues, cells were examined morphologically under a light microscope throughout the entire treatment period. No signs of cytotoxicity or stress-related changes (*e.g.*, cell rounding, detachment, or granulation) were observed at any of the tested concentrations. After 24 h of treatment, the cell supernatant was removed, and the cells were lysed for a period of 5 min at RT with 60 μL of Tropix lysis solution (Applied Biosystems). The cell lysate was stored at −80°C until further processing. Luciferase activity was determined by adding 100 μL of a D-luciferin substrate solution into 20 μL of the lysate in pure grade white 96-well microtiter plates (BRAND, Wertheim, Germany). The luciferin solution consisted of 0.56 mM D-luciferin, 63 mM ATP, 0.27 mM CoA, 0.13 mM EDTA, 33.3 mM dithiothreitol, and 8 mM $MgSO_4$. The luminescence was then measured with the SpectraMax L Microplate Reader (Molecular Devices, San Jose, CA, USA). The respective β-galactosidase activity was quantified with the same plates and device using 20 μL of the lysate and the Galacto-Light Plus™ kit (Applied Biosystems). The luciferase activity of each well was normalized to the respective β-galactosidase activity.

2.4. Computational modeling

The crystal structure of the ERα (PDB ID 4MGD) (Delfosse et al. 2014) was downloaded and pre-processed for further analyses assuming pH 7.4 ± 0.5 using the protein preparation wizard in Schrödinger (version 2024–3; Protein Preparation Workflow; Epik; Impact; Prime; Schrödinger, LLC, New York, NY, 2024). This crystal structure was chosen based on its high resolution (1.9 Å), specifically around the ligand HPTE (bisphenol-class compound) featuring a bulky trifluoromethyl group. This structure presumably provides a more suitable receptor conformation for accommodating the voluminous linker of BPTMC than the crystal structure with bound BPA (PDB ID 3UU7). Missing loops were filled with Prime, and protonation states were calculated with Epik. S-hydroxycysteine (CSO) residues were mutated back to cysteines, and Ser537, a mutation introduced for crystallization, was mutated back to the original residue Tyr537. To obtain a complex with BPA, Glide docking (standard precision) was used (Friesner et al. 2004). To obtain a complex with BPTMC, Dolina flexible docking was employed, due to the larger size of BPTMC compared to HPTE (Smiesko, 2013). The best ranked poses were selected for further processing.

The protein-ligand complexes were neutralized by adding counterions and solvated in TIP3P water (orthorhombic box, 10 Å). A salt concentration of 0.15 M was added and minimization was carried out using the OPLS_2005 force field. The system was equilibrated using the standard protocol of Desmond (version 2023–4; Desmond Molecular Dynamics System, D. E. Shaw Research, New York, NY, 2023. Maestro-Desmond Interoperability Tools, Schrödinger, New York, NY, 2023). Then, three replicate molecular dynamics (MD) simulations of 50 ns were performed for both complexes, using the default settings of Desmond (version 2023–4). In total, 1000 frames were written out for each simulation. Ligand root mean square fluctuation (RMSF) was calculated

for the atoms of the bisphenol core structure (excluding substituents on the bridge). The RMSF reflects the standard deviation in specified atom position during the MD trajectory and is calculated following Eq. 1 (Tsukamoto et al. 2024):

$$RMSF = \sqrt{\left\langle (r_i - \langle r_i \rangle)^2 \right\rangle} \quad (1)$$

where r_i is the position of atom i and $\langle r_i \rangle$ is the ensemble average position of atom i. In this case, a high RMSF value indicates large fluctuations in the position of the bisphenol core atoms during the simulation, which means more movement of the bisphenol core in the binding pocket of ERα.

For every MD simulation, the binding free energy was calculated with thermal MM/GBSA script (Schrödinger, version 2024–3). For the calculation, frames 100–500 were selected to allow for a short equilibration period, and a step size of 10 was used. From the MM/GBSA data, the desolvation energy was extracted by taking the negative of the solvation energy. Values were reported as the mean ± SD. Lastly, Qikprop (Version 2024–3; QikProp, Schrödinger, LLC, New York, NY, 2024) was used to calculate basic physico-chemical descriptors of BPA and BPTMC.

2.5. 17β-HSD1 activity assay

The 17β-HSD1 activity was determined as described previously, with some modifications (Engeli et al. 2017). Briefly, 2×10^6 HEK-293 cells were seeded per 10 cm dish in 10 mL medium, left to attach for 18 h and transiently transfected with 8 μg of plasmid for human 17β-HSD1 using a modified version of the calcium phosphate precipitation method (Graham and van der Eb, 1973). The plasmid DNA was diluted in 37°C water to a final volume of 437.5 μL/dish. A volume of 62.5 μL/dish of 37°C 2 M $CaCl_2$ was added slowly. The mixture was pipetted dropwise into an equal volume of 37°C 2x BEST solution (described above in Section 2.3) and incubated at RT for 15 min. The cells were transfected by adding 1 mL/dish of the prepared DNA-$CaCl_2$-BEST transfection mixture to the culture medium. After a period of 4 h the medium containing the transfection mix was removed and replaced with fresh medium (10 mL/dish). After a 48 h period following transfection, cells were collected in 2 mL ice cold PBS, then portioned in 200 μL aliquots and pelleted for 4 min at 13,000 g at 4°C prior to snap freezing in liquid nitrogen and storage at −80°C. For each experiment, cell pellets were resuspended in 1 mL TS2 buffer (100 mM NaCl, 1 mM EGTA, 1 mM EDTA, 1 mM $MgCl_2$, 250 mM sucrose, 20 mM Tris HCl, pH 7.4) and lysed by sonication (UP50H sonicator, Hielscher Ultrasonics). Cell lysates were diluted to obtain 30 % substrate to product conversion after a 10 min incubation. The diluted HEK-293 cell lysate (10 μL) containing overexpressed 17β-HSD1 was pre-incubated with either DMSO as solvent control or DMSO-dissolved test compound diluted in TS2 buffer in a total volume of 12.2 μL for 8 min on ice. The total solvent concentration in the reaction was 0.1 %. The reaction was started by adding 10 μL of a reaction mixture containing substrate and co-substrate. 17β-HSD1 activity was determined in the presence of 200 nM E1 in TS2 buffer, including 81 pCi/μL of [6,7–3H]-estrone (Anawa) and 454 μM NADPH. The reaction mixture was incubated for 10 min at 37°C, after which the reaction was terminated with 10 μL pure methanol containing 5 mM E1 and 5 mM E2. 10 μL of each sample was applied to TLC plates (Macherey Nagel, Oensingen, Switzerland), and steroids were separated using a mobile phase consisting of chloroform and ethyl acetate in a 4:1 ratio. The plates were dried overnight, bands of E1 and E2 were visualized under UV light, marked, excised, and analyzed via scintillation counting using a Tri-Carb 2900TR liquid scintillation analyzer (Packard, Meriden, Connecticut, USA) with the IRGASAFE Plus scintillation cocktail (Zinsser Analytic, Eschborn, Germany). To determine the enzymatic activity of 17β-HSD1, the conversion rate of E1 to E2 was calculated and normalized to the DMSO control.

2.6. 17β-HSD2 activity assay

17β-HSD2 activity was determined as described previously, with some modifications (Engeli et al. 2017). Briefly, 2×10^6 HEK-293 cells were seeded per 10 cm dish in 10 mL medium, left to attach for 18 h and transiently transfected with 8 μg of plasmid for human 17β-HSD2 as described above for 17β-HSD1, followed by preparation of cell pellets that were stored at −80°C. For activity assays, cell pellets were resuspended in 1 mL TS2 buffer and diluted to obtain 30 % conversion. The diluted HEK-293 cell lysate (10 μL) containing overexpressed 17β-HSD2 was pre-incubated with either DMSO as solvent control or DMSO-dissolved test compound diluted in TS2 buffer in a total volume of 12.2 μL for 8 min on ice. The total solvent concentration in the reaction was 0.1 %. The reaction was started by adding 10 μL of the substrate and co-substrate. 17β-HSD2 activity was determined in the presence of 200 nM E2 in TS2 buffer, including 3 Bq/μL (81 pCi/μL) of [2,4,6,7–3H]-estradiol (PerkinElmer) and 454 μM NAD^+. The reaction mixture was incubated for 10 min at 37°C, followed by termination of the reaction by adding 10 μL methanol containing 5 mM E1 and 5 mM E2. 10 μL of each sample was applied to TLC plates (Macherey Nagel), and steroids were separated using a mobile phase consisting of chloroform and ethyl acetate in a 4:1 ratio. The plates were dried overnight, bands of E1 and E2 were visualized under UV light, marked, excised, and analyzed via scintillation counting using a Tri-Carb 2900TR liquid scintillation analyzer (Packard) with the IRGASAFE Plus scintillation cocktail (Zinsser Analytic). To determine the enzymatic activity of 17β-HSD2, the conversion rate of E2 to E1 was calculated and normalized to the DMSO control.

2.7. Quantification of mRNA by RT-qPCR

MCF-7 cells were seeded in a 6-well plate in normal culture medium at a density of 450,000 cells/well and allowed to attach overnight. To deprive the cells of steroids, the medium was replaced 4 h prior to treatment with phenol-red-free DMEM with high glucose (4.5 g/L) (Sigma-Aldrich), 10 mM HEPES, pH 7.4 (BioConcept), supplemented with 10 % FBS (Biowest) that was charcoal-treated as described above (Section 2.3). Treatment was initiated by replacing the steroid-free medium with the treatment medium which consisted of the same steroid-deprived medium but contained the compounds of interest at the desired concentration as well as 0.1 % DMSO. Following a 24 h treatment period, the cells were washed with ice-cold PBS and then frozen at −80°C. MCF-7 cells were lysed with 350 μL of RLT buffer (Qiagen, Hombrechtikon, Switzerland) and the cell lysate was transferred to RNeasy® Plus Mini gDNA eliminator columns and then centrifuged for 1 min at 13,000 g. From the eluate, total RNA was extracted according to the manufacturer (Qiagen RNeasy® Plus Mini Extraction kit). We assessed the RNA concentration and quality using a NanoDrop 2000 (Thermo Scientific). cDNA was synthesized from 1 μg RNA using PrimeScript RT Reagent Kit (Takara Bio Europe SAS; Saint-Germain-en-Laye, France) according to the manufacturer. The real-time PCR measurement of individual cDNAs was performed in triplicate using SYBR green dye (Roche Diagnostics, Rotkreuz, Switzerland) containing 10 μM of each primer (sense and antisense) (see Suppl. Table 1). Relative mRNA levels were calculated using the $\Delta\Delta C_t$ method with *Peptidylprolyl isomerase A* (*PPIA*) as housekeeping gene (Tsachaki et al. 2020).

2.8. Real-time cell proliferation assay

MCF-7 cells were seeded in a 96-well plate in normal culture medium at a density of 5,000 cells per well and allowed to attach overnight. Cells were treated in phenol-red-free DMEM with high glucose (4.5 g/L; Sigma-Aldrich) supplemented with 10 % steroid-depleted FBS (Biowest). For the steroid depletion, the FBS was charcoal-treated as described in Section 2.3. To deprive the cells of steroids before the start of the treatment, medium was replaced with the steroid-deprived

medium 3 h prior to treatment. The 3 h steroid deprivation was optimized to reduce background estrogenic activity and sensitize cells to E2, while maintaining cell viability and avoiding stress from extended culture in charcoal-stripped, phenol red-free medium. The concentration of DMSO did not exceed 0.1 % in the treatment medium and was maintained at a constant level across all treatments. After starting the treatment, the cells were monitored for 72 h with the Celloger Mini Plus™ (Curiosis, Seoul, South Korea). The confluency of the cells was determined with the CellogerAnalysis App Version 2.1.2023.0512 (Curiosis). The doubling time was calculated with a non-linear fit (exponential growth equation) in GraphPad Prism 10.2.0. (GraphPad Software, La Jolla, CA, USA). Each treatment was measured in three biological replicates with six technical replicates each.

2.9. Statistical analysis

Data are given as mean ± SD of at least three independent experiments. Statistical analyses were performed using the GraphPad Prism 10.2.0. One-way analysis of variance (ANOVA) was then used for comparisons between groups, followed by Tukey or Dunnett's post-test procedure to localize differences between treatments containing chemicals and the vehicle group. Concentration response curves for estimation of half-maximal inhibitory concentration (IC_{50}) values were fitted and analyzed by non-linear regression. Statistical significance was set at * $p < 0.05$.

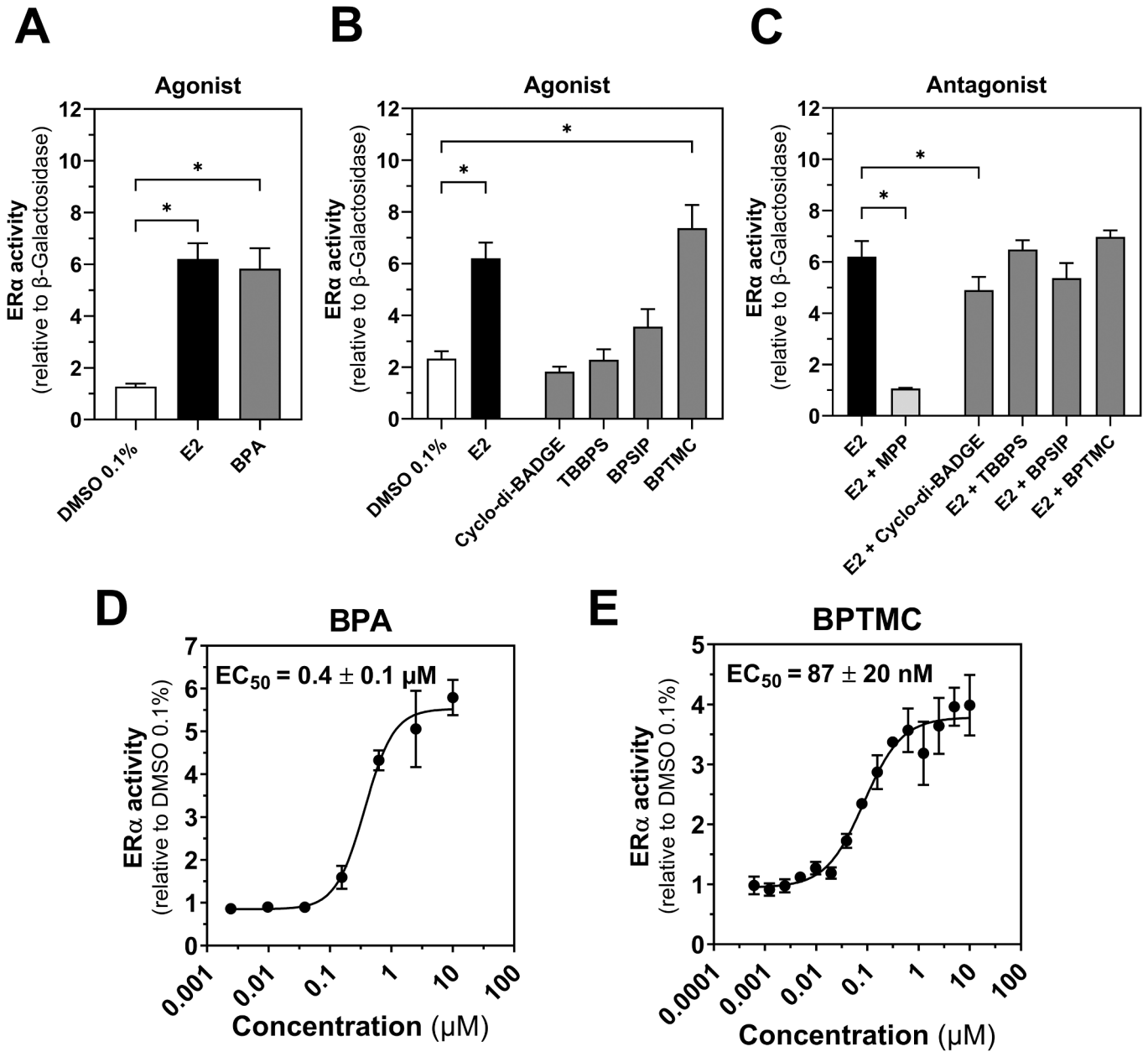

Fig. 2. Screening of BPA and its analogues for ERα agonistic and antagonistic activity. (**A**) ERα agonistic activity of 10 µM BPA. E2 was used at 2 nM as positive control. (**B**) Screening of the BPA analogues cyclo-di-BADGE, TBBPS, BPSIP, and BPTMC at 10 µM for ERα agonistic effects. (**C**) Screening of the BPA analogues cyclo-di-BADGE, TBBPS, BPSIP, and BPTMC at 10 µM for ERα antagonistic effects in the presence of 2 nM E2. The selective ERα antagonist MPP was used at 2.5 µM as a positive control. (**D**) EC_{50} curve of BPA on ERα agonistic activity. (**E**) EC_{50} curve of BPTMC on ERα agonistic activity. Values represent mean ± SD of three independent experiments, each performed in technical duplicates. Statistical significance was determined using one-way ANOVA, followed by Dunnett's post-test with *$p < 0.05$.

3. Results

3.1. BPTMC is a significantly more potent ERα activator than BPA

To assess the estrogenic activity of BPA and its four analogues, we conducted luciferase reporter gene measurements using HEK-293 cells transiently expressing human ERα, a responsive luciferase construct and β-galactosidase as transfection control for normalization. Each compound was first tested at a concentration of 10 μM to evaluate both agonistic and antagonistic effects on ERα, using a cell-based transactivation assay. As shown in Fig. 2A, BPA activated ERα in a clear agonistic response, confirming the findings of earlier studies (Gould et al. 1998). Among the analogues, BPTMC also induced ERα-dependent transactivation to a level comparable to the 2 nM E2 positive control, whereas cyclo-di-BADGE, TBBPS, and BPSIP showed no significant agonistic activity (Fig. 2B). In the presence of 2 nM E2, MPP at 2.5 μM was used as positive control for a selective ERα antagonist. Our screening revealed that cyclo-di-BADGE at 10 μM exhibited weak antagonistic activity (Fig. 2C). However, no concentration-dependent effect was observed in a follow-up quantification (data not shown). Notably, while BPTMC functioned as an ERα agonist, it did not further enhance the reporter gene activity in the presence of 2 nM E2, suggesting maximal activation of the reporter gene (Fig. 2C). For BPA, no relevant antagonistic effect on ERα has been observed at concentrations below 100 μM (Delfosse et al. 2012; Durcik et al. 2022; Lee et al. 2023); therefore, it was not further investigated in our study. To quantify the relative potencies of BPA and BPTMC as ERα agonists, we conducted concentration-response experiments and determined their half-maximal effective concentrations (EC_{50}). BPA showed an EC_{50} of 0.4 ± 0.1 μM (Fig. 2D), while BPTMC demonstrated a significantly lower EC_{50} of 87 ± 20 nM (Fig. 2E). Our findings indicate that BPTMC is significantly more potent than BPA in activating ERα.

3.2. Increased binding stability and lipophilicity enhance BPTMC's ERα interaction

To investigate how subtle structural differences between BPA and BPTMC affect their binding affinity to ERα, their physicochemical properties and binding poses were compared. As shown in Table 1, BPTMC showed a higher lipophilicity (logP), lower solubility (logS), and a smaller dipole moment than BPA, indicating greater overall hydrophobicity. This was further supported by the calculated desolvation energies ($\Delta G_{desolvation}$): BPTMC presented a 3.8 kcal/mol lower desolvation cost than BPA, suggesting a more favorable transfer from the solvent to the lipophilic ERα binding pocket. These results indicate that increased hydrophobicity of BPTMC contributes to its enhanced binding affinity for ERα.

Next, the stability of BPA and BPTMC during MD simulations was compared. Fig. 3A shows the initial binding pose of BPA at the start of the simulation. Notably, all crystal docked BPA poses formed interactions with Glu353 and Thr347. However, in the published crystal structure of BPA to ERα (PDB ID 3UU7; (Delfosse et al. 2012)), the compound is oriented with its bridge directed away from Phe404 and interacts instead with the thioether acceptor of Met421 rather than hydroxyl oxygen of Thr347 (Suppl. Figure 1). The electron density around His524 in 3UU7 is weak, while some density is observed near Thr347, suggesting that BPA may adopt two alternative binding poses. In all three MD simulations, the interaction with Thr347 was consistently maintained. However, the interaction with Glu353 was repeatedly lost (Fig. 3B).

BPTMC adopted a similar binding pose to BPA (Fig. 3C). Unlike BPA, BPTMC maintained stable interactions with both Thr347 and Glu353 throughout the simulation. This increased stability is likely due to the bulkier substituent on its bridge, which limits ligand flexibility and mobility, thus anchoring the molecule firmly within the ERα binding pocket. The calculated average RMSF confirmed this higher stability of

Table 1
Property overview (calculated with QikProp) and desolvation energy (average calculated from three replicate MD simulations with MM/GBSA) for BPA and BPTMC.

Compound	BPA	BPTMC
LogP	3.3	4.5
LogS	-3.4	-5.6
Dipole moment [Debye]	2.1	1.2
ΔG_{bind} (kcal/mol)	-50.2 ± 3.5	-65.2 ± 5.5
$\Delta G_{desolvation}$ (kcal/mol)	-18.2 ± 1.3	-22.0 ± 2.0

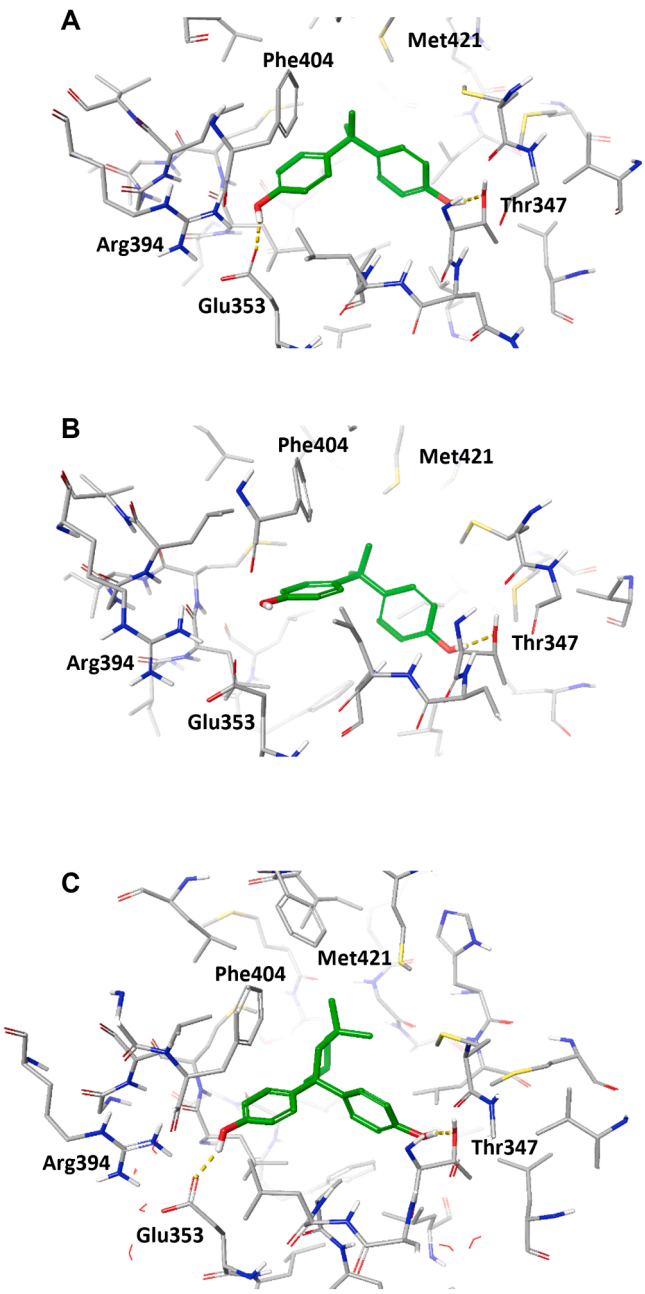

Fig. 3. Molecular dynamics of BPA and BPTMC binding to ERα. (**A**) BPA (green) bound to ERα at the start of MD simulations, forming hydrogen bonds (yellow dashed lines) with Glu353 and Thr347. (**B**) BPA (green) during MD simulations, losing interaction with Glu353. (**C**) BPTMC (green) bound to ERα, forming hydrogen bonds with Glu353 and Thr347. Images were generated in Schrödinger Maestro (2024–3).

the bisphenol core, with an average of 0.94 ± 0.06 Å for BPTMC compared to 1.19 ± 0.07 Å for BPA. Additionally, the larger ring structure of BPTMC enabled more extensive van der Waals interactions with surrounding lipophilic residues (Met343, Met421, Leu525, Leu540), whereas BPA did not fully exploit the lipophilic potential of the available cavity. The lower stability of BPA in the ERα binding pocket was further reflected by its higher binding free energy (ΔG_{bind}) compared to BPTMC, as shown in Table 1.

3.3. BPTMC, but not BPA, shows moderate inhibition of 17β-HSD2

To investigate whether the BPA derivatives might interfere with the enzymes controlling the intracellular concentrations of active estrogens, we assessed their ability to inhibit the key steroid-converting enzymes 17β-HSD1 and 17β-HSD2. Initial screening assays were conducted at a compound concentration of 10 μM to evaluate potential enzyme inhibition (Figs. 4A and 4B). Compounds leading to less than 30 % residual enzymatic activity were selected for determining the IC_{50}. As expected, the positive controls apigenin and NDGA (Engeli et al. 2017) used at a concentration of 20 μM resulted in a significant inhibition of 17β-HSD1 and 17β-HSD2 activities, respectively (Figs. 4A and 4B). Interestingly, BPA at 10 μM did not alter the activity of either 17β-HSD1 or 17β-HSD2. In addition, none of the tested BPA analogues significantly inhibited 17β-HSD1 activity, although BPTMC showed a tendency towards lowering its activity (Fig. 4A). Cyclo-di-BADGE, TBBPS, and BPSIP did also not elicit substantial inhibition of 17β-HSD2 activity (Fig. 4B). Although TBBPS and BPSIP caused a statistically significant decrease in 17β-HSD2 activity, the residual enzymatic activity remained above 30 % (Fig. 4B). In contrast, BPTMC markedly inhibited 17β-HSD2, reducing enzyme activity to below 20 % at a concentration of 10 μM. The concentration-response analysis of BPTMC revealed a moderate inhibitory potency with an IC_{50} value of 4.8 ± 0.6 μM (Fig. 4C).

3.4. BPTMC upregulates the expression of ERα downstream target genes in MCF-7 breast cancer cells

To assess the transcriptional activity of ERα in a pathophysiologically relevant cellular context, we employed MCF-7 cells, a well-established, ERα-positive human breast cancer cell line. MCF-7 cells are widely used as a model system for studying estrogenic signaling due to their endogenous expression of functional ERα and their sensitivity to E2 (Hamelers et al. 2003). In particular, ERα activation in MCF-7 cells has been shown to induce the expression of canonically estrogen-responsive genes such as *Growth regulation by estrogen in breast cancer 1* (*GREB1*), *Trefoil factor 1*, also known as *pS2* (*TFF1*), and *Progesterone receptor* (*PGR*), all of which are established transcriptional targets of ERα (Duijndam et al. 2021).

Cell viability was first assessed using the colorimetric XTT assay. As shown in Suppl. Figure 2, the positive control (0.1 % Triton-X) decreased viability of MCF-7 cells. Notably, we found that viability was not significantly affected by exposure to BPTMC for 24 h up to 3 μM (Suppl. Figure 2).

To evaluate whether BPTMC can upregulate the expression of ERα target genes, MCF-7 cells were exposed to increasing concentrations (8 nM to 1 μM) of BPTMC, and mRNA levels of *GREB1* (Fig. 5A), *TFF1* (Fig. 5B), and *PGR* (Fig. 5C) were quantified by RT-qPCR. Treatment with 1 μM BPTMC for 24 h resulted in a marked upregulation of all three ERα-regulated genes, with expression levels comparable to those observed following exposure to the positive control 10 nM E2. Notably, an increase in *TFF1* mRNA levels was detectable at concentrations as low as 200 nM BPTMC, indicating a concentration-dependent estrogenic response. To confirm that the transcriptional activation was specifically mediated via ERα, co-treatment experiments were conducted using the selective ERα antagonist fulvestrant at 100 nM. Co-administration of fulvestrant with either 10 nM E2 or 1 μM BPTMC substantially attenuated the induction of the expression of *GREB1*, *TFF1*, and *PGR*,

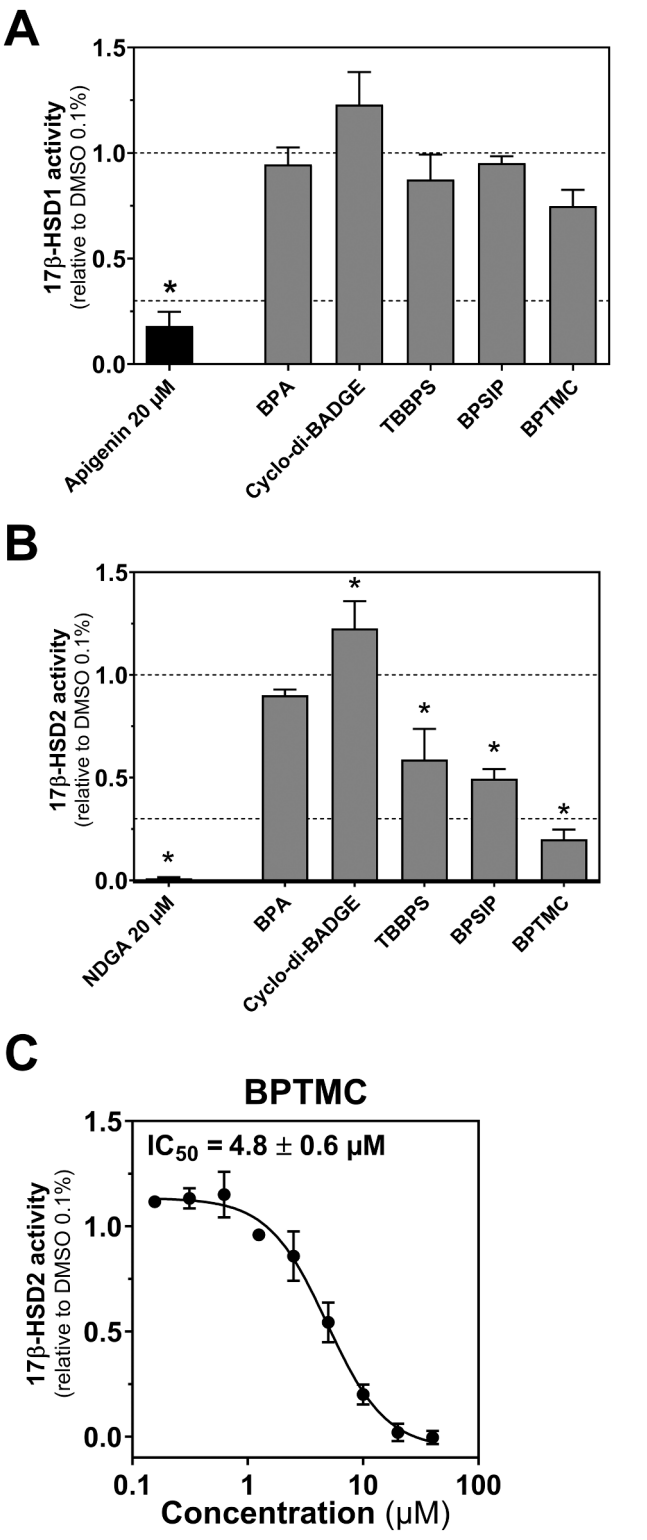

Fig. 4. Screening for 17β-HSD1 and 17β-HSD2 inhibitory activity by BPA and its analogues. (**A**) 17β-HSD1 inhibitory activity of 10 μM BPA, cyclo-di-BADGE, TBBPS, BPSIP, and BPTMC was measured in lysates of 17β-HSD1-transfected HEK-293 cells. 20 μM apigenin served as positive control for inhibition. (**B**) 17β-HSD2 inhibitory activity of 10 μM BPA, cyclo-di-BADGE, TBBPS, BPSIP, and BPTMC was measured in lysates of 17β-HSD2 transfected HEK-293 cells. 20 μM NDGA served as positive control for inhibition. (**C**) IC_{50} curve for 17β-HSD2 inhibition by BPTMC. An IC_{50} value of 4.8 ± 0.6 μM was obtained. Values represent mean ± SD of three independent experiments, each performed in technical duplicates. Statistical significance was determined using one-way ANOVA, followed by Dunnett's post-test, with *$p < 0.05$.

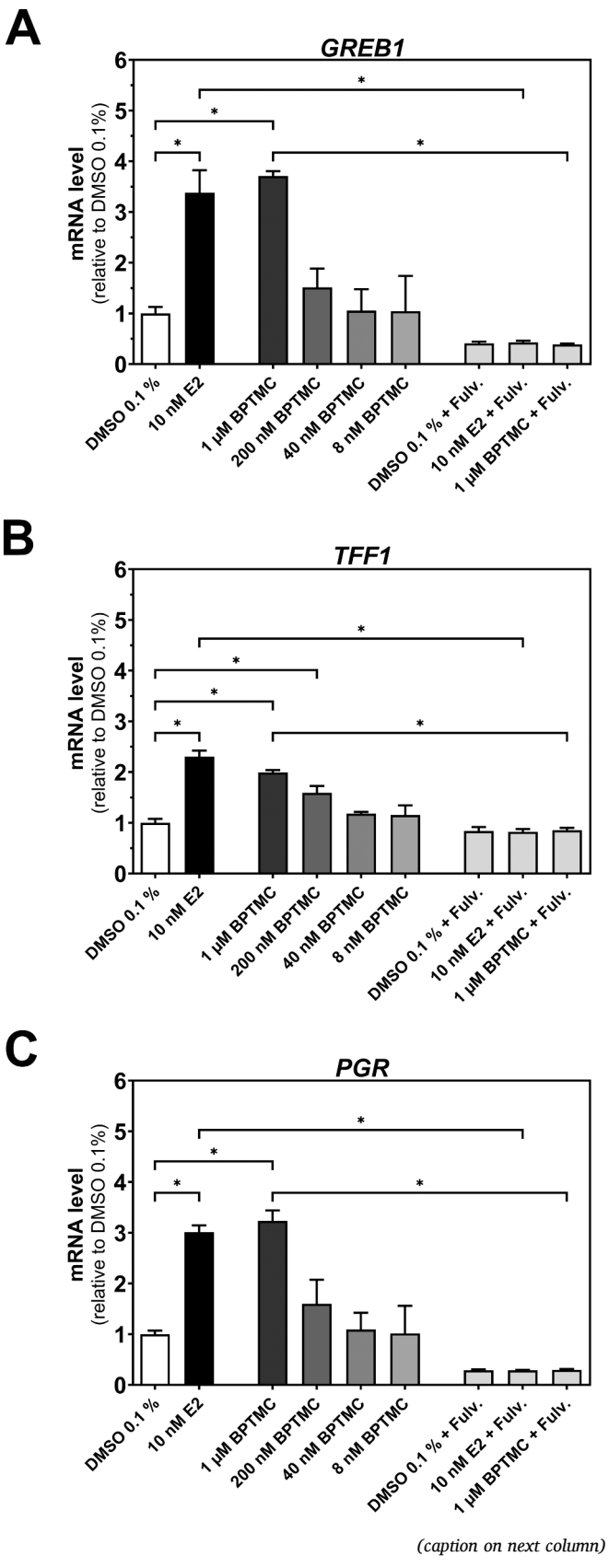

(caption on next column)

Fig. 5. mRNA levels of three downstream targets of ERα in MCF-7 breast cancer cells after exposure to various concentrations of BPTMC for 24 h. (**A**) mRNA levels of *GREB1* after 24 h exposure to the indicated concentrations of BPTMC. 10 nM E2 was used as a positive control for ERα activation. The increase in *GREB1* mRNA levels induced by E2 or BPTMC exposure was blocked by 100 nM of the selective ERα antagonist fulvestrant. (**B**) mRNA levels of *TFF1* after 24 h exposure to various concentrations of BPTMC. 10 nM E2 was used as a positive control for ERα activation. The increase in *TFF1* mRNA levels induced by E2 or BPTMC exposure was blocked by 100 nM fulvestrant. (**C**) mRNA levels of *PGR* after 24 h exposure to various concentrations of BPTMC. 10 nM E2 was used as a positive control for ERα activation. The increase in *PGR* mRNA levels induced by E2 or BPTMC exposure was blocked by 100 nM fulvestrant. Values represent mean ± SD of three independent experiments, each performed in technical triplicates. Statistical significance was determined using one-way ANOVA, followed by Tukey's post-test, with *p < 0.05.

confirming that the effects of BPTMC were ERα-dependent (Figs. 5A, 5B, and 5C). These results demonstrate that BPTMC can upregulate estrogenic gene expression in ERα-positive breast cancer cells, supporting its classification as an ERα agonist.

3.5. Low nanomolar concentrations of BPTMC promote proliferation of MCF-7 breast cancer cells

To evaluate the proliferative effects of BPTMC on ERα-positive cells, we monitored MCF-7 breast cancer cell proliferation, following treatment with various concentrations of BPTMC, 10 nM E2 as positive control, or vehicle negative control. Cell proliferation was assessed over a 72 h period by measuring confluency (Fig. 6) and impedance (Suppl. Figure 3) in the steroid-deprived treatment medium, both of which are established indicators of cell growth and density. The endpoint of the cell proliferation was further validated by performing a cell count after the 72-h treatment period (Suppl. Figure 4). MCF-7 cells treated with vehicle control showed minimal proliferation, with confluency plateauing between 20 and 30 h post-treatment (Fig. 6A). In contrast, treatment with 10 nM E2 (Figs. 6B), 1 µM BPTMC (Fig. 6C), or 100 nM BPTMC (Fig. 6D) resulted in sustained cell proliferation over the full 72 h period, culminating in significantly increased confluency and cell count compared to vehicle-treated cells (Fig. 6I and Suppl. Figure 4). These findings indicate that BPTMC stimulates MCF-7 cell proliferation in a concentration-dependent manner, with 100 nM being sufficient to elicit a significant mitogenic effect. These results were confirmed in impedance-based monitoring (Suppl. Figure 3). Notably, 72 h exposure at 100 nM resulted in a greater increase in cell number with BPTMC than with BPA (Suppl. Figure 4). At 10 nM BPTMC, no clear increase in confluency and cell number was observed (Fig. 6E and Suppl. Figure 4), suggesting that this concentration may be below the threshold required to drive robust cell proliferation. However, impedance-based monitoring revealed more ambiguous results at 10 nM (Suppl. Figures 3E and 3I), potentially indicating low-level or context-dependent proliferative activity not captured by assessing confluency and cell count. To confirm that the observed proliferative effects were indeed mediated by ERα activation, co-treatment experiments were performed using 100 nM of the selective ERα antagonist fulvestrant. Co-treatment with fulvestrant abolished the proliferative response to 10 nM E2 (Fig. 6G and Suppl. Figure 4), 1 µM BPTMC (Fig. 6H and Suppl. Figure 4), and 1 µM BPA (Suppl. Figure 4). Confluency and cell number in these groups remained comparable to those of the vehicle and fulvestrant control group (Fig. 6F and Suppl. Figure 4). The impedance-based monitoring confirmed that BPTMC-induced MCF-7 cell proliferation is ERα-dependent (Suppl. Figure 3).

As a next step, the corresponding doubling time for each condition was calculated (Suppl. Figure 5). The doubling time of control MCF-7 cells was 50.9 ± 8.1 h, which aligns well with the literature (Ruohola et al. 2001). Exposure to 10 nM E2 reduced the doubling time by approximately two-fold, consistent with the well-known

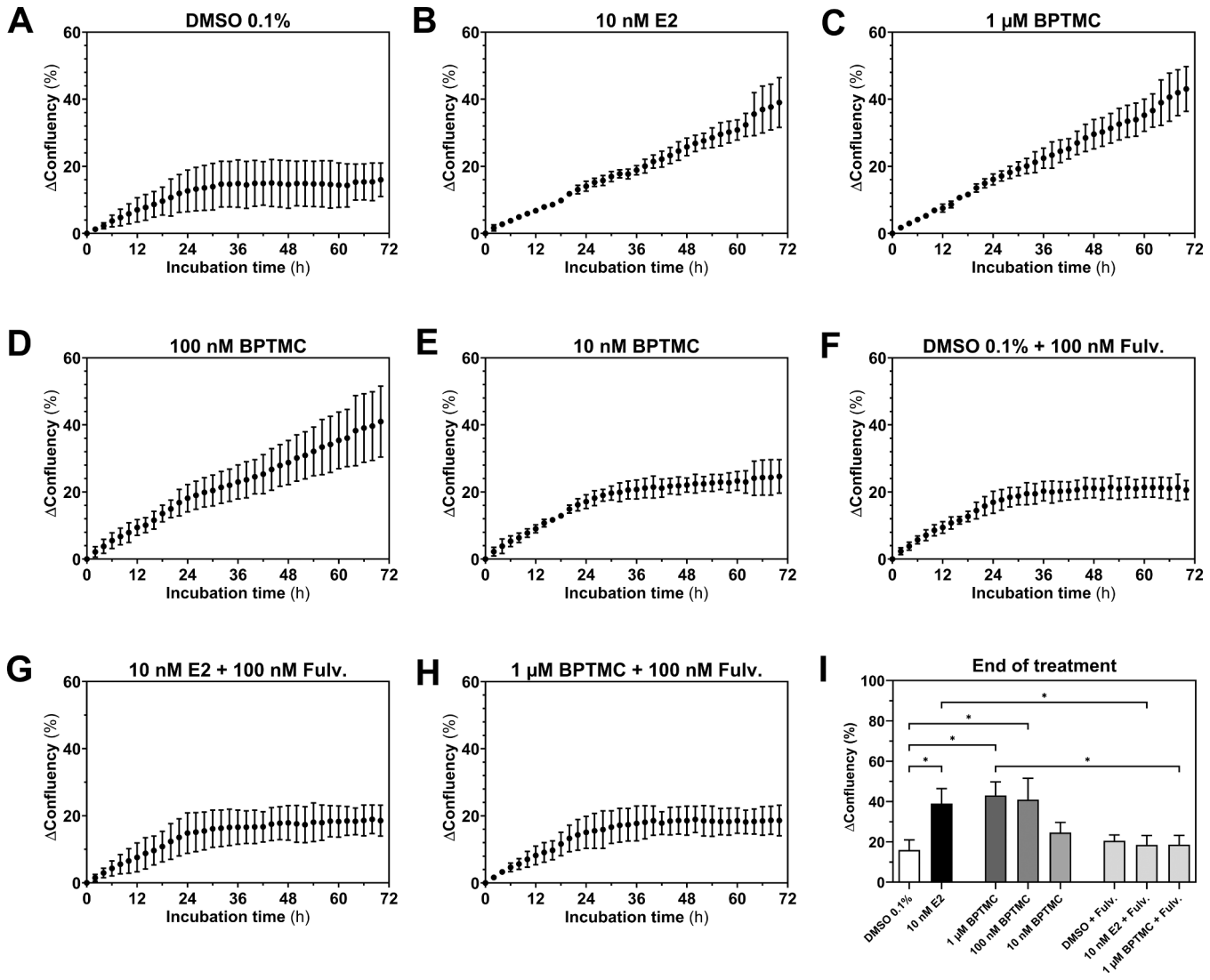

Fig. 6. MCF-7 cell proliferation in response to BPTMC. The difference in confluency (ΔConfluency) at the timepoint of measurement compared to the start of the treatment was quantified. (**A-E**) Confluency progression of MCF-7 cells in (**A**) DMSO 0.1 %, (**B**) 10 nM E2 as positive control for estrogen-mediated increase in cell proliferation, as well as (**C**) 1 µM, (**D**) 100 nM and (**E**) 10 nM BPTMC. (**F-H**) Confluency progression of MCF-7 cells with 100 nM of the selective ERα antagonist fulvestrant to mitigate estrogenic effects: (**F**) DMSO 0.1 %, (**G**) 10 nM E2, and (**H**) 1 µM BPTMC. (**I**) ΔConfluency at the end of the 72 h treatment period. Values represent mean ± SD of three independent experiments, each performed in six technical replicates. Statistical significance was determined using one-way ANOVA, followed by Tukey's post-test, with *p < 0.05.

estrogen-induced proliferative response. Similarly, treatment with BPTMC at 100 nM and 1 µM decreased the doubling time, whereas 10 nM BPTMC had no noticeable effect (Suppl. Figure 5). Importantly, co-treatment with fulvestrant reversed the doubling time of both E2- and BPTMC-treated cells to that of vehicle treated MCF-7 cells, confirming that the proliferative effects are mediated through ERα (Suppl. Figure 5). Taken together, these findings demonstrate that BPTMC promotes the proliferation of ERα-positive breast cancer cells at nanomolar concentrations, highlighting its potential estrogenic and pro-proliferative properties in hormone-sensitive tissues.

4. Discussion

The transactivation assays performed in HEK-293 cells expressing human ERα and a responsive luciferase reporter construct revealed that BPTMC is a significantly more potent ERα agonist than BPA. In contrast, BPSIP tended to activate ERα at 10 µM, whereas cyclo-di-BADGE and TBBPS were inactive. None of the four compounds tested exhibited antagonistic activity towards ERα. Molecular modeling further showed that BPTMC possessed higher lipophilicity, lower solubility, and a smaller dipole moment than BPA, indicating greater overall hydrophobicity. Consequently, binding of BPTMC to the ERα ligand-binding site released more $\Delta G_{desolvation}$, thereby strengthening ligand-receptor interactions. This enhanced interaction may be a possible explanation for the observed increase in ERα activation potency compared to BPA. Interestingly, BPTMC, but not BPA, was found to be a moderate inhibitor of the E2-inactivating 17β-HSD2, which could lead to elevated local E2 concentrations, thus enhancing local ERα activation. Importantly, BPTMC strongly upregulated the expression of the ERα target genes *GREB1*, *TFF1*, and *PGR*, starting at nanomolar concentrations in the MCF-7 breast cancer cell line, which endogenously expresses ERα. The magnitude of gene induction was comparable to that elicited by 10 nM E2 and was completely abrogated by the ERα antagonist fulvestrant, confirming receptor-specific activation. Consistent with its transcriptional activity, BPTMC also promoted proliferation of MCF-7 cells at nanomolar concentrations, an effect similarly reversed by fulvestrant. Collectively, these findings identify BPTMC as potent ERα agonist, with additional inhibitory activity against the E2-inactivating enzyme 17β-

HSD2. However, additional effects on other nuclear receptors and steroid metabolizing enzymes remain to be clarified.

The European Chemicals Agency (ECHA) has classified BPA as a "substance of very high concern" due to its endocrine-disrupting properties and reproductive toxicity (den Braver-Sewradj et al. 2020). In line with European Union regulatory frameworks, BPA and several of its derivatives have demonstrated endocrine-disrupting effects, which are of particular concern for sensitive populations such as pregnant and breastfeeding women, given the importance of estrogens in the development of reproductive and mammary gland systems (Beausoleil et al. 2018). A body of evidence has linked BPA exposure to a broad range of adverse health outcomes, including developmental, metabolic, reproductive, immunological, and oncogenic effects (Rochester, 2013). As a result, BPA has been subjected to increasingly stringent regulatory restrictions and partial bans. Nonetheless, the rapid introduction of functional BPA substitutes, often without robust toxicological evaluation, raises concerns of "regrettable substitutions", wherein replacement compounds may pose equal or even greater health hazards. Although efforts to assess BPA alternatives have intensified and regulatory agencies, including the European Commission, have emphasized the need for comprehensive and transparent safety assessments (European_Commission 2024), substantial knowledge gaps remain. The ongoing phase-out of BPA and related compounds, driven by new restrictions within the European Union, has accelerated the demand for functionally equivalent replacements (European_Commission 2024). Among the emerging alternatives, BPTMC has already been identified as a candidate BPA substitute and prioritized for toxicological evaluation (van den Brand et al., 2024). Like BPA, BPTMC has been detected in both environmental and human biomonitoring samples (Franko et al. 2024; Lucarini et al. 2020; Sauer et al. 2021). Its detection in 55 % of baby bottles sold in Canada as of 2021 underscores its growing commercial relevance and potential for widespread exposure (Siddique et al. 2021). Despite its increasing use, BPTMC remains poorly studied in terms of endocrine activity and systemic toxicity. Other BPA replacements have raised similar concerns. BPSIP, introduced as a dye-developing agent in thermal paper, has limited biomonitoring data available. However, it was detected in thermal paper receipts in Switzerland at concentrations ranging from 3.4 to 13.2 mg/g (Goldinger et al. 2015). Notably, BPSIP was more frequently detected in blood samples than BPA and bisphenol S (BPS), suggesting greater persistence and potential for systemic exposure (Thayer et al. 2016). Cyclo-di-BADGE, a degradation product or polymerization byproduct that is not covalently bound within polymer networks, is prone to migration into food. In this context, cyclo-di-BADGE and other BADGE derivatives have been identified in canned food samples (Bustos et al. 2023). TBBPS is a flame retardant and has been found globally in various environmental media. While it is used as an alternative to tetrabromobisphenol A (TBBPA), scientific opinion suggests that TBBPS and its derivatives may not be entirely environment friendly. Studies indicate that TBBPS can cause various toxic effects, including neurotoxicity, hepatotoxicity, and cytotoxicity (Xu et al. 2024). Despite the increasing prevalence of these BPA analogues in consumer products and the environment, toxicological data remain limited (Pelch et al. 2019).

Given the structural similarities among bisphenol derivatives (Fig. 1) and their demonstrated bioactivities, only a limited number of studies have assessed their estrogenic activity. In this study, we confirmed the ERα agonistic effect of BPA. This aligns with previous findings demonstrating that BPA can compete with the natural ligand E2 for binding to the ligand-binding pocket (LBP) of ERα (Delfosse et al. 2012; Paris et al. 2002). Although the estrogenic potency of BPA is significantly lower than that of E2, it has been shown to elicit estrogenic responses *in vivo* through direct interaction with ERα (Matthews et al. 2001). While extensive data exist for BPA and its most common replacements (*e.g.,* BPS, bisphenol F (BPF), bisphenol AF (BPAF)), information on many other bisphenol analogues and substitution candidates remains sparse, inconsistent, or entirely lacking (Pelch et al. 2019). Earlier studies have assessed estrogenic effects of some BPA replacement compounds using MCF-7 breast cancer cells. For most of the studied compounds, ERα-mediated estrogenic effects were observed either alone or in mixtures. Notably, BPAF, bisphenol B (BPB), BPF, BPS, bisphenol Z (BPZ), tetrachlorobisphenol A (TCBPA), and tetramethylbisphenol A (TMBPA) exhibited estrogenic activity at the mid- and high nanomolar range, comparable to or exceeding that of BPA (Bockers et al. 2020; Kim et al. 2017; Kitamura et al. 2005; Matteo et al. 2025; Zhao et al. 2019). In contrast, bisphenol P (BPP), diphenylmethane (DPM), diphenylpropane (DPP), tetramethylbisphenol F (TMBPF), Pergafast 201, and 2,4′-BPS showed no detectable activation of ERα-mediated signaling (Kitamura et al. 2005; Matteo et al. 2025). Studies of bisphenolic mixtures suggested that their estrogenic effects are largely additive (Matteo et al. 2025).

In this context, our study provides novel evidence that BPTMC exhibits potent estrogenic activity in human cell-based systems, with robust ERα activation observed at mid-nanomolar concentrations. To the best of our knowledge, this is the first study demonstrating such pronounced estrogenic effects of BPTMC in physiologically relevant models. This is especially relevant considering that the less potent BPA has been restricted for its endocrine-disrupting properties. This finding contrasts earlier reports that either showed minimal ERα activation by BPTMC or identified only weak estrogenic effects in the micromolar range (Dvorakova et al. 2018; Elke Eilebrecht et al., 2019; Keminer et al. 2020). These discrepancies may reflect differences in assay sensitivity, cell model relevance, or the use of non-physiological exposure levels. Our results underscore the importance of employing human-derived cell systems and realistic concentration ranges when evaluating endocrine activity. Our *in silico* analysis of BPA and BPTMC binding shows that hydrophobicity and pose rigidity affected binding affinity to ERα. This suggests that broader virtual screening of bisphenol properties might be beneficial to identify BPA derivatives with estrogenic activity. ERα is widely distributed throughout the body, in a variety of tissues. ERα is expressed primarily in the uterus, mammary glands, liver, kidneys, skeletal muscles, and heart (Couse and Korach, 1999). It is also expressed in the epididymis, thyroid, bones, adrenals (Brandenberger et al. 1997; Pau et al. 1998), and certain regions of the brain (Couse and Korach, 1999), as well as granulosa cells (dependent on follicle stage), ovarian surface epithelium, and theca cells (Saunders et al. 2000). E2 plays a critical role in many physiological processes in both females and males. These include normal growth, development, and cell-type-specific gene regulation in tissues of the reproductive tract, central nervous system, and skeleton (Chen et al. 2022). Since BPTMC is a potent ERα agonist, it may interfere with estrogen-regulated physiological processes, potentially leading to adverse effects in both central and peripheral systems.

In addition to its estrogenic properties, BPTMC has been reported to exert strong anti-progestagenic and weak anti-androgenic effects in transgenic human U2-OS osteosarcoma cells (Sauer et al. 2021). Moreover, comparative cytotoxicity assessments have revealed that BPTMC induces marked cell death in various reproductive cell models, including C18–4 spermatogonial cells (7.9 μM), steroidogenic MA-10 (Leydig) cells (4.5 μM), and KGN (granulosa) cells (14.7 μM), often with greater potency than BPA or other bisphenol analogues (Rajkumar et al. 2021). In contrast, we did not observe any cytotoxicity in MCF-7 cells (15,000 cells/well) exposed for 24 h to BPTMC at concentrations up to 3 μM. The apparent discrepancy (particularly for Leydig cells) may be explained by experimental differences, including cell type, lower cell density (2, 000–6,000 cells/well), serum composition, and longer exposure duration (48 h), likely accounting for the cytotoxic responses observed by Rajkumar et al. (2021). Notably, yeast-based reporter assays have detected ERα agonism by BPTMC only at relatively high concentrations (*e.g.,* EC_{10} = 4 μM and EC_{50} = 3 μM) (Dvorakova et al. 2018; van Leeuwen et al. 2019), suggesting lower sensitivity of these systems and further underscoring the need of mammalian cell-based models to evaluate endocrine activity. Assuming a scenario where BPTMC

eventually reaches tissue concentrations comparable to pre-regulation BPA levels, relevant testing concentrations would likely fall in the low nanomolar range. For example, BPA levels in breast adipose tissue of breast cancer patients have been measured at 4.2 ng/g, translating to ~17 nM when adjusted for tissue density and molecular weight (Baldwin et al. 2010; Keshavarz-Maleki et al. 2021). Tissue concentrations of BPA are generally higher in lipid-rich compartments and can reach up to 50-fold higher in fetal tissues, reflecting its lipophilic nature and potential for bioaccumulation (Geens et al. 2012; Nahar et al. 2015). Although human exposure data for BPTMC remain very limited, its higher lipophilicity compared with BPA suggests a potentially greater tissue accumulation (Zhao et al. 2023). The only reported plasma concentration of BPTMC is 0.014 μg/L (~45 pM) with reported values ranging from non-detectable levels up to 0.207 μg/L (~ 0.7 nM) (Hu et al. 2025), while urinary levels were below detection (Lucarini et al. 2020). Based on BPA data, where adipose tissue concentrations are approximately 4–5 times higher than plasma, and considering that BPA can reach up to 50-fold higher levels in certain fetal tissues, a similar concentration might be expected for BPTMC. Applying the 4–5x tissue-to-plasma ratio to the highest reported human plasma level (0.7 nM) yields estimated BPTMC concentrations of ~3–4 nM in lipid-rich tissues, and potentially up to ~30–35 nM in fetal compartments. Given that the *in vitro* EC_{50} for BPTMC is 87 nM, these estimated tissue levels fall within an order of magnitude of the biologically active concentrations determined in our MCF-7 assays, where ERα-mediated gene activation and proliferation were observed. Although industrial production of BPTMC seems to be increasing considerably, no data are currently available on annual production of BPTMC or its concentrations in animals although it has been detected in environmental samples (Sauer et al. 2021). This highlights the urgent need for systematic biomonitoring in both human and environmental matrices for BPTMC.

For other BPA derivatives, the available data remain incomplete or inconclusive. For example, BPSIP has shown no detectable ERα activity in human assays (Keminer et al. 2020), while TBBPS, despite computational predictions of ERα binding, exhibited such high cytotoxicity that functional evaluation was not feasible (Cao et al. 2017). Cyclo-di-BADGE, to our knowledge, has not yet been tested for ERα modulation and did not show robust agonistic or antagonistic activity against ERα in our study.

The estrogenic effect of BPA appears to be receptor-mediated, as it did not inhibit 17β-HSD2 that inactivates E2 and its inhibitory effects on 17β-HSD1 ($IC_{50} > 100$ μM, (Chen et al. 2023)) requires concentrations far exceeding those found in biomonitoring studies, suggesting limited toxicological relevance. However, structurally related analogues may exhibit much higher potencies for enzyme inhibition. For instance, TBBPA inhibits 17β-HSD1 at nanomolar concentrations, representing a 100-fold higher potency than BPA (Chen et al. 2023). We corroborated these findings experimentally, observing nanomolar IC_{50} values of TBBPA against 17β-HSD1 (data not shown). While several BPA derivatives have been shown to inhibit steroidogenic enzymes such as 3β-HSD2 or 17β-HSD1 (Chen et al. 2023; Chen et al. 2024), such inhibitory effects could not be observed for cyclo-di-BADGE, TBBPS, BPSIP, or BPTMC at concentrations up to 10 μM in the present study. Nevertheless, this emphasizes the importance to include steroid-metabolizing enzymes in the analysis of endocrine-disrupting substances.

Recent evidence from a study using isolated granulosa cells suggested that BPTMC may influence steroid hormone production by altering gene expression (mRNA levels) of *HSD3B2* and modulating the secretion of progesterone and E2 (Iskandarani et al., 2025). Animal studies face limitations in translating findings to humans due to interspecies differences in metabolic pathways, as exemplified by species-specific variations in 17β-HSD1 inhibition by BPA (Ye et al. 2011). *In vitro* systems are useful alternatives but face their own challenges, such as the lack of metabolic capacity. Future improvements may include co-culture models incorporating metabolizing cells or the use of hepatic S9 fractions to simulate biotransformation.

17β-HSD2 catalyzes the oxidation of active 17β-hydroxy sex steroids into their less active or inactive 17-keto forms, including the conversion of E2 to E1, and testosterone to androstenedione, thereby exerting a protective function in peripheral tissues by preventing excessive local activity of these potent hormones (Moghrabi et al. 1997; Tsachaki and Odermatt, 2019). Data on the modulation of 17β-HSD2 by BPA and its substitutes remain scarce. Our results indicate that BPA does not inhibit 17β-HSD2 and has a very low affinity to interact with the catalytic site. The two BPA analogs TBBPS and BPSIP partially inhibited 17β-HSD2 activity at 10 μM, suggesting a moderate interaction with the enzyme. BPTMC inhibited 17β-HSD2 activity with an IC_{50} of approximately 5 μM, exceeding the concentrations found in environmental and human samples and raising questions regarding the toxicological relevance of this observation. By inhibiting 17β-HSD2, BPTMC could promote elevated local concentrations of E2 in peripheral tissues, which could enhance estrogen-dependent effects or pathologies, particularly in hormone-sensitive tissues. However, because ERα agonistic activity of BPTMC occurs at nanomolar concentrations, while 17β-HSD2 inhibition requires micromolar levels, significant enzyme inhibition is unlikely at concentrations relevant for ERα activation. Thus, the primary mechanism underlying the endocrine-disrupting potential of BPTMC includes most likely direct activation of ERα. Nonetheless, at higher exposure levels, 17β-HSD2 inhibition may still contribute to the overall endocrine-disrupting profile of BPTMC, potentially in an additive or synergistic manner, especially under complex exposure scenarios involving mixtures of BPA analogues.

In conclusion, our findings establish BPTMC as a potent ERα agonist, capable of inducing both transcriptional activity and mitogenic responses at low, nanomolar concentrations. This potency raises significant concerns regarding its potential as an EDC, particularly given its increasing use as a BPA substitute in consumer products. The observed biological activity of BPTMC at relevant concentrations suggests potential interference with hormone-regulated processes, including those involved in reproductive and developmental health, as well as hormone-responsive breast cancer, as indicated by its effects in MCF-7 cells, or endometriosis and endometrial cancer (not addressed in this study). Given these findings, BPTMC warrants further attention in toxicological evaluations and regulatory frameworks. Its emerging presence in products such as baby bottles, combined with the lack of comprehensive exposure data, highlights the urgency of further research into its pharmacokinetics, metabolism, and long-term health effects. Future studies on BPTMC should prioritize comprehensive toxicokinetic investigations, including the application of physiologically-based toxicokinetic (PBTK) models to better predict internal exposures across different populations and life stages. In parallel, research should also examine tissue-specific biological responses, potential cumulative or synergistic effects with other EDCs, and identify particularly vulnerable windows of susceptibility, such as prenatal and early postnatal development, when exposure may have long-lasting or irreversible consequences. In the broader context of chemical substitution policy, BPTMC exemplifies the risks associated with insufficiently tested BPA alternatives. These results underscore the critical need for a rigorous, mechanism-based screening strategy including comprehensive *in silico* characterization to evaluate replacement compounds before widespread adoption. Identifying structurally diverse, well-characterized, and biologically inert alternatives should be a top priority, not only to protect public health but also to ensure that regulatory efforts do not inadvertently perpetuate or exacerbate the very risks they aim to mitigate.

CRediT authorship contribution statement

Manuel Kley: Writing – review & editing, Visualization. **Jamal Bouitbir:** Writing – review & editing, Writing – original draft, Supervision, Resources, Project administration, Funding acquisition, Conceptualization. **Alex Odermatt:** Writing – review & editing, Writing

– original draft, Supervision, Resources, Project administration, Funding acquisition, Conceptualization. **Marie-Christin Jäger:** Writing – review & editing, Visualization. **Martin Smieško:** Writing – original draft, Supervision, Software. **Rianne E. van Diest:** Writing – original draft, Investigation, Formal analysis, Data curation. **Friedrich L. Joos:** Writing – review & editing, Writing – original draft, Visualization, Validation, Investigation, Formal analysis, Data curation.

Declaration of Competing Interest

The authors declare the following financial interests/personal relationships that may be considered potential competing interests: Alex Odermatt and Jamal Bouitbir report financial support from the Swiss Centre for Applied Human Toxicology. The other authors declare that they have no competing financial interests or personal relationships that could have influenced the work reported in this paper.

Acknowledgement

This work was supported by the Swiss Centre for Applied Human Toxicology (SCAHT) to AO (No. SCAHT-GL 21–06) and JB (No. RV-AV 23–01). We thank Anne-Laure Demierre, Sabine Frey, and Orlando Mani from the Swiss Federal Office of Public Health (FOPH) for their valuable contributions to the discussion.

Appendix A. Supporting information

Supplementary data associated with this article can be found in the online version at doi:10.1016/j.tox.2025.154393.

Data availability

Data will be made available on request.

References

Arnal, J.F., Lenfant, F., Metivier, R., Flouriot, G., Henrion, D., Adlanmerini, M., Fontaine, C., Gourdy, P., Chambon, P., Katzenellenbogen, B., Katzenellenbogen, J., 2017. Membrane and Nuclear Estrogen Receptor Alpha Actions: From Tissue Specificity to Medical Implications. Physiol. Rev. 97, 1045–1087.

Baldwin, C.J., Kelly, E.J., Batchelor, A.G., 2010. The variation in breast density and its relationship to delayed wound healing: a prospective study of 40 reduction mammoplasties. J. Plast. Reconstr. Aesthet. Surg. 63, 663–665.

Beausoleil, C., Emond, C., Cravedi, J.P., Antignac, J.P., Applanat, M., Appenzeller, B.R., Beaudouin, R., Belzunces, L.P., Canivenc-Lavier, M.C., Chevalier, N., Chevrier, C., Elefant, E., Eustache, F., Habert, R., Kolf-Clauw, M., Le Magueresse-Battistoni, B., Mhaouty-Kodja, S., Minier, C., Multigner, L., Schroeder, H., Thonneau, P., Viguie, C., Pouzaud, F., Ormsby, J.N., Rousselle, C., Verines-Jouin, L., Pasquier, E., Michel, C., 2018. Regulatory identification of BPA as an endocrine disruptor: Context and methodology. Mol. Cell Endocrinol. 475, 4–9.

Becker, K., Goen, T., Seiwert, M., Conrad, A., Pick-Fuss, H., Muller, J., Wittassek, M., Schulz, C., Kolossa-Gehring, M., 2009. GerES IV: phthalate metabolites and bisphenol A in urine of German children. Int J. Hyg. Environ. Health 212, 685–692.

Bockers, M., Paul, N.W., Efferth, T., 2020. Bisphenolic compounds alter gene expression in MCF-7 cells through interaction with estrogen receptor alpha. Toxicol. Appl. Pharm. 399, 115030.

Brandenberger, A.W., Tee, M.K., Lee, J.Y., Chao, V., Jaffe, R.B., 1997. Tissue distribution of estrogen receptors alpha (ER-alpha) and beta (ER-beta) mRNA in the midgestational human fetus. J. Clin. Endocrinol. Metab. 82, 3509–3512.

Bruni, V., Capozzi, A., Lello, S., 2022. The Role of Genetics, Epigenetics and Lifestyle in Polycystic Ovary Syndrome Development: the State of the Art. Reprod. Sci. 29, 668–679.

Bustos, J., Lestido-Cardama, A., Santillana, M.I., Sendón, R., Paseiro Losada, P., Rodríguez Bernaldo de Quirós, A., 2023. Quantification of Cyclo-di-BADGE and Identification of Several BADGE Derivatives in Canned Food Samples. Coatings 13, 792.

Calafat, A.M., Ye, X., Wong, L.Y., Reidy, J.A., Needham, L.L., 2008. Exposure of the U.S. population to bisphenol A and 4-tertiary-octylphenol: 2003-2004. Environ. Health Perspect. 116, 39–44.

Cao, H., Wang, F., Liang, Y., Wang, H., Zhang, A., Song, M., 2017. Experimental and computational insights on the recognition mechanism between the estrogen receptor alpha with bisphenol compounds. Arch. Toxicol. 91, 3897–3912.

Chen, P., Li, B., Ou-Yang, L., 2022. Role of estrogen receptors in health and disease. Front Endocrinol. (Lausanne) 13, 839005.

Chen, S., Wang, S., Zheng, J., Lu, H., Chen, H., Tang, Y., Wang, N., Zhu, Y., Wang, Y., Duan, P., Ge, R.S., 2023. Bisphenol analogues inhibit human and rat 17beta-hydroxysteroid dehydrogenase 1: 3D-quantitative structure-activity relationship (3D-QSAR) and in silico docking analysis. Food Chem. Toxicol. 181, 114052.

Chen, Y., Zhang, H., Yu, Y., Wang, S., Wang, M., Pan, C., Fei, Q., Li, H., Wang, Y., Lv, J., Ge, R.S., 2024. Comparison of structure-activity relationship for bisphenol analogs in the inhibition of gonadal 3beta-hydroxysteroid dehydrogenases among human, rat, and mouse. J. Steroid Biochem Mol. Biol. 236, 106424.

Couse, J.F., Korach, K.S., 1999. Estrogen receptor null mice: what have we learned and where will they lead us? Endocr. Rev. 20, 358–417.

Cull, M.E., Winn, L.M., 2024. Bisphenol A and its potential mechanism of action for reproductive toxicity. Toxicology 511, 154040.

Delfosse, V., Grimaldi, M., Cavailles, V., Balaguer, P., Bourguet, W., 2014. Structural and functional profiling of environmental ligands for estrogen receptors. Environ. Health Perspect. 122, 1306–1313.

Delfosse, V., Grimaldi, M., Pons, J.L., Boulahtouf, A., le Maire, A., Cavailles, V., Labesse, G., Bourguet, W., Balaguer, P., 2012. Structural and mechanistic insights into bisphenols action provide guidelines for risk assessment and discovery of bisphenol A substitutes. Proc. Natl. Acad. Sci. USA 109, 14930–14935.

den Braver-Sewradj, S.P., van Spronsen, R., Hessel, E.V.S., 2020. Substitution of bisphenol A: a review of the carcinogenicity, reproductive toxicity, and endocrine disruption potential of alternative substances. Crit. Rev. Toxicol. 50, 128–147.

Deroo, B.J., Korach, K.S., 2006. Estrogen receptors and human disease. J. Clin. Invest 116, 561–570.

Diamanti-Kandarakis, E., Bourguignon, J.P., Giudice, L.C., Hauser, R., Prins, G.S., Soto, A.M., Zoeller, R.T., Gore, A.C., 2009. Endocrine-disrupting chemicals: an Endocrine Society scientific statement. Endocr. Rev. 30, 293–342.

Duenas-Moreno, J., Mora, A., Kumar, M., Meng, X.Z., Mahlknecht, J., 2023. Worldwide risk assessment of phthalates and bisphenol A in humans: The need for updating guidelines. Environ. Int 181, 108294.

Duijndam, B., Goudriaan, A., van den Hoorn, T., van der Stel, W., Le Devedec, S., Bouwman, P., van der Laan, J.W., van de Water, B., 2021. Physiologically Relevant Estrogen Receptor Alpha Pathway Reporters for Single-Cell Imaging-Based Carcinogenic Hazard Assessment of Estrogenic Compounds. Toxicol. Sci. 181, 187–198.

Durcik, M., Hiti, L., Tomasic, T., Masic, L.P., 2022. New bisphenol A and bisphenol S analogs: Evaluation of their hERalpha agonistic and antagonistic activities using the OECD 455 in-vitro assay and molecular modeling. Chem. Biol. Inter. 354, 109820.

Dvorakova, M., Kejlova, K., Rucki, M., Jirova, D., 2018. Selected bisphenols and phthalates screened for estrogen and androgen disruption by in silico and in vitro methods. Neuro Endocrinol. Lett. 39, 409–416.

Elke Eilebrecht, A.W., Matthias Teigeler, Björn Windshügel, Oliver Keminer, Laura Chachulski, Manfred Kohler. 2019. Bewertung des endokrinen Potenzials von Bisphenol Alternativstoffen in umweltrelevanten Verwendungen. In: B. Fraunhofer Institut für Molekularbiologie und Angewandte Oekologie and S.F.I. Angewandte Ökologie (IME-AE), Bereich Screening Port (SP), Hamburg (Eds), Umweltbundesamt.

Engeli, R.T., Rohrer, S.R., Vuorinen, A., Herdlinger, S., Kaserer, T., Leugger, S., Schuster, D., Odermatt, A., 2017. Interference of Paraben Compounds with Estrogen Metabolism by Inhibition of 17beta-Hydroxysteroid Dehydrogenases. Int J. Mol. Sci. 18.

European_Commission. 2024. COMMISSION REGULATION (EU) 2024/3190 of 19 December 2024. On the use of bisphenol A (BPA) and other bisphenols and bisphenol derivatives with harmonised classification for specific hazardous properties in certain materials and articles intended to come into contact with food, amending Regulation (EU) No 10/2011 and repealing Regulation (EU) 2018/213. In: E. Union (Ed), Official Journal of the European Union.

Franko, N., Kodila, A., Sollner Dolenc, M., 2024. Adverse outcomes of the newly emerging bisphenol A substitutes. Chemosphere 364, 143147.

Friesner, R.A., Banks, J.L., Murphy, R.B., Halgren, T.A., Klicic, J.J., Mainz, D.T., Repasky, M.P., Knoll, E.H., Shelley, M., Perry, J.K., Shaw, D.E., Francis, P., Shenkin, P.S., 2004. Glide: a new approach for rapid, accurate docking and scoring. 1. Method and assessment of docking accuracy. J. Med Chem. 47, 1739–1749.

Geens, T., Neels, H., Covaci, A., 2012. Distribution of bisphenol-A, triclosan and n-nonylphenol in human adipose tissue, liver and brain. Chemosphere 87, 796–802.

Goldinger, D.M., Demierre, A.L., Zoller, O., Rupp, H., Reinhard, H., Magnin, R., Becker, T.W., Bourqui-Pittet, M., 2015. Endocrine activity of alternatives to BPA found in thermal paper in Switzerland. Regul. Toxicol. Pharm. 71, 453–462.

Gould, J.C., Leonard, L.S., Maness, S.C., Wagner, B.L., Conner, K., Zacharewski, T., Safe, S., McDonnell, D.P., Gaido, K.W., 1998. Bisphenol A interacts with the estrogen receptor alpha in a distinct manner from estradiol. Mol. Cell Endocrinol. 142, 203–214.

Government_of_Canada. 2023. Risk management action milestones for bisphenol A. Government of Canada.

Graham, F.L., van der Eb, A.J., 1973. A new technique for the assay of infectivity of human adenovirus 5 DNA. Virology 52, 456–467.

Hamelers, I.H., Van Schaik, R.F., Sussenbach, J.S., Steenbergh, P.H., 2003. 17beta-Estradiol responsiveness of MCF-7 laboratory strains is dependent on an autocrine signal activating the IGF type I receptor. Cancer Cell Int 3, 10.

Hassan, S., Thacharodi, A., Priya, A., Meenatchi, R., Hegde, T.A., R, T., Nguyen, H.T., Pugazhendhi, A., 2024. Endocrine disruptors: Unravelling the link between chemical exposure and Women's reproductive health. Environ. Res 241, 117385.

Hilborn, E., Stal, O., Jansson, A., 2017. Estrogen and androgen-converting enzymes 17beta-hydroxysteroid dehydrogenase and their involvement in cancer: with a special focus on 17beta-hydroxysteroid dehydrogenase type 1, 2, and breast cancer. Oncotarget 8, 30552–30562.

Hoekstra, E.J., Simoneau, C., 2013. Release of bisphenol A from polycarbonate: a review. Crit. Rev. Food Sci. Nutr. 53, 386–402.
Hu, G., Zhang, Z., Huang, Y., Fang, D., Zhan, M., Qu, W., Zhou, Y., 2025. Development of a sensitive UPLC-MS/MS method for simultaneous determination of 15 Bisphenol A analogues in human serum and urine: Application of paired samples and global exposure assessment. J. Chromatogr. A 1760, 466217.
Iskandarani, L., Romanelli, S., Hales, B.F., Robaire, B., 2025. The Effects of Bisphenol A and its Analogs on Steroidogenesis in MA-10 Leydig Cells and KGN Granulosa Cellsdagger. Biol Reprod 112, 399–414.
Keminer, O., Teigeler, M., Kohler, M., Wenzel, A., Arning, J., Kassner, F., Windshugel, B., Eilebrecht, E., 2020. A tiered high-throughput screening approach for evaluation of estrogen and androgen receptor modulation by environmentally relevant bisphenol A substitutes. Sci. Total Environ. 717, 134743.
Keshavarz-Maleki, R., Kaviani, A., Omranipour, R., Gholami, M., Khoshayand, M.R., Ostad, S.N., Sabzevari, O., 2021. Bisphenol-A in biological samples of breast cancer mastectomy and mammoplasty patients and correlation with levels measured in urine and tissue. Sci. Rep. 11, 18411.
Khan, N., Sharma, K.K., Andersson, S., Auchus, R.J., 2004. Human 17beta-hydroxysteroid dehydrogenases types 1, 2, and 3 catalyze bi-directional equilibrium reactions, rather than unidirectional metabolism, in HEK-293 cells. Arch. Biochem Biophys. 429, 50–59.
Kim, J.Y., Choi, H.G., Lee, H.M., Lee, G.A., Hwang, K.A., Choi, K.C., 2017. Effects of bisphenol compounds on the growth and epithelial mesenchymal transition of MCF-7 CV human breast cancer cells. J. Biomed. Res 31, 358–369.
Kiss, S.J., 2013. Legislation by Agenda-Setting: Assessing the Media's Role in the Regulation of Bisphenol A in the U.S. States. Mass Commun. Soc. 16, 687–712.
Kitamura, S., Suzuki, T., Sanoh, S., Kohta, R., Jinno, N., Sugihara, K., Yoshihara, S., Fujimoto, N., Watanabe, H., Ohta, S., 2005. Comparative study of the endocrine-disrupting activity of bisphenol A and 19 related compounds. Toxicol. Sci. 84, 249–259.
Lee, H., Park, J., Park, K., 2023. Mixture Effects of Bisphenol A and Its Structural Analogs on Estrogen Receptor Transcriptional Activation. Toxics 11.
Lucarini, F., Krasniqi, T., Bailat Rosset, G., Roth, N., Hopf, N.B., Broillet, M.C., Staedler, D., 2020. Exposure to New Emerging Bisphenols Among Young Children in Switzerland. Int J. Environ. Res Public Health 17.
Manzoor, M.F., Tariq, T., Fatima, B., Sahar, A., Tariq, F., Munir, S., Khan, S., Nawaz Ranjha, M.M.A., Sameen, A., Zeng, X.A., Ibrahim, S.A., 2022. An insight into bisphenol A, food exposure and its adverse effects on health: A review. Front Nutr. 9, 1047827.
March, W.A., Moore, V.M., Willson, K.J., Phillips, D.I., Norman, R.J., Davies, M.J., 2010. The prevalence of polycystic ovary syndrome in a community sample assessed under contrasting diagnostic criteria. Hum. Reprod. 25, 544–551.
Matteo, G., Cho, E., Rigden, M., Eickmeyer, D.C., Bradford, L.M., Meier, M.J., Williams, A., Corton, J.C., Yauk, C.L., Atlas, E., 2025. High-throughput transcriptomics analysis of equipotent and human relevant mixtures of BPA alternatives reveal additive effects in vitro. Arch. Toxicol. 99, 3707–3719.
Matthews, J.B., Twomey, K., Zacharewski, T.R., 2001. In vitro and in vivo interactions of bisphenol A and its metabolite, bisphenol A glucuronide, with estrogen receptors alpha and beta. Chem. Res Toxicol. 14, 149–157.
Mercogliano, R., Santonicola, S., 2018. Investigation on bisphenol A levels in human milk and dairy supply chain: A review. Food Chem. Toxicol. 114, 98–107.
Michalowicz, J., 2014. Bisphenol A–sources, toxicity and biotransformation. Environ. Toxicol. Pharm. 37, 738–758.
Miettinen, M.M., Mustonen, M.V., Poutanen, M.H., Isomaa, V.V., Vihko, R.K., 1996. Human 17 beta-hydroxysteroid dehydrogenase type 1 and type 2 isoenzymes have opposite activities in cultured cells and characteristic cell- and tissue-specific expression. Biochem J. 314 (Pt 3), 839–845.
Mlynarcikova, A., Fickova, M., Scsukova, S., 2014. Impact of endocrine disruptors on ovarian steroidogenesis. Endocr. Regul. 48, 201–224.
Moghrabi, N., Head, J.R., Andersson, S., 1997. Cell type-specific expression of 17 beta-hydroxysteroid dehydrogenase type 2 in human placenta and fetal liver. J. Clin. Endocrinol. Metab. 82, 3872–3878.
Mustieles, V., D'Cruz, S.C., Couderq, S., Rodriguez-Carrillo, A., Fini, J.B., Hofer, T., Steffensen, I.L., Dirven, H., Barouki, R., Olea, N., Fernandez, M.F., David, A., 2020. Bisphenol A and its analogues: A comprehensive review to identify and prioritize effect biomarkers for human biomonitoring. Environ. Int 144, 105811.
Nahar, M.S., Liao, C., Kannan, K., Harris, C., Dolinoy, D.C., 2015. In utero bisphenol A concentration, metabolism, and global DNA methylation across matched placenta, kidney, and liver in the human fetus. Chemosphere 124, 54–60.
Neuvonen, R., Huovinen, M., Dorman, D.C., Laitinen, H., Sahlman, H., 2023. Phthalates and polycystic ovary syndrome - Systematic literature review. Reprod. Toxicol. 121, 108473.
Odermatt, A., Strajhar, P., Engeli, R.T., 2016. Disruption of steroidogenesis: Cell models for mechanistic investigations and as screening tools. J. Steroid Biochem Mol. Biol. 158, 9–21.
Paris, F., Balaguer, P., Terouanne, B., Servant, N., Lacoste, C., Cravedi, J.P., Nicolas, J.C., Sultan, C., 2002. Phenylphenols, biphenols, bisphenol-A and 4-tert-octylphenol exhibit alpha and beta estrogen activities and antiandrogen activity in reporter cell lines. Mol. Cell Endocrinol. 193, 43–49.
Pau, C.Y., Pau, K.Y., Spies, H.G., 1998. Putative estrogen receptor beta and alpha mRNA expression in male and female rhesus macaques. Mol. Cell Endocrinol. 146, 59–68.
Pelch, K., Wignall, J.A., Goldstone, A.E., Ross, P.K., Blain, R.B., Shapiro, A.J., Holmgren, S.D., Hsieh, J.H., Svoboda, D., Auerbach, S.S., Parham, F.M., Masten, S. A., Walker, V., Rooney, A., Thayer, K.A., 2019. A scoping review of the health and toxicological activity of bisphenol A (BPA) structural analogues and functional alternatives. Toxicology 424, 152235.
Peltoketo, H., Vihko, P., Vihko, R., 1999. Regulation of estrogen action: role of 17 beta-hydroxysteroid dehydrogenases. Vitam. Horm. 55, 353–398.
Poutanen, M., Isomaa, V., Lehto, V.P., Vihko, R., 1992a. Immunological analysis of 17 beta-hydroxysteroid dehydrogenase in benign and malignant human breast tissue. Int J. Cancer 50, 386–390.
Poutanen, M., Moncharmont, B., Vihko, R., 1992b. 17 beta-hydroxysteroid dehydrogenase gene expression in human breast cancer cells: regulation of expression by a progestin. Cancer Res 52, 290–294.
Rajkumar, A., Luu, T., Beal, M.A., Barton-Maclaren, T.S., Robaire, B., Hales, B.F., 2021. Elucidation of the Effects of Bisphenol A and Structural Analogs on Germ and Steroidogenic Cells Using Single Cell High-Content Imaging. Toxicol. Sci. 180, 224–238.
Rochester, J.R., 2013. Bisphenol A and human health: a review of the literature. Reprod. Toxicol. 42, 132–155.
Ruohola, J.K., Viitanen, T.P., Valve, E.M., Seppanen, J.A., Loponen, N.T., Keskitalo, J.J., Lakkakorpi, P.T., Harkonen, P.L., 2001. Enhanced invasion and tumor growth of fibroblast growth factor 8b-overexpressing MCF-7 human breast cancer cells. Cancer Res 61, 4229–4237.
Sauer, P., Svecova, H., Grabicova, K., Gonul Aydin, F., Mackulak, T., Kodes, V., Blytt, L. D., Henninge, L.B., Grabic, R., Kocour Kroupova, H., 2021. Bisphenols emerging in Norwegian and Czech aquatic environments show transthyretin binding potency and other less-studied endocrine-disrupting activities. Sci. Total Environ. 751, 141801.
Saunders, P.T., Millar, M.R., Williams, K., Macpherson, S., Harkiss, D., Anderson, R.A., Orr, B., Groome, N.P., Scobie, G., Fraser, H.M., 2000. Differential expression of estrogen receptor-alpha and -beta and androgen receptor in the ovaries of marmosets and humans. Biol. Reprod. 63, 1098–1105.
Schug, T.T., Janesick, A., Blumberg, B., Heindel, J.J., 2011. Endocrine disrupting chemicals and disease susceptibility. J. Steroid Biochem Mol. Biol. 127, 204–215.
Seachrist, D.D., Bonk, K.W., Ho, S.M., Prins, G.S., Soto, A.M., Keri, R.A., 2016. A review of the carcinogenic potential of bisphenol A. Reprod. Toxicol. 59, 167–182.
Siddique, S., Zhang, G., Coleman, K., Kubwabo, C., 2021. Investigation of the migration of bisphenols from baby bottles and sippy cups. Curr. Res Food Sci. 4, 619–626.
Sieck, N.E., Bruening, M., van Woerden, I., Whisner, C., Payne-Sturges, D.C., 2024. Effects of Behavioral, Clinical, and Policy Interventions in Reducing Human Exposure to Bisphenols and Phthalates: A Scoping Review. Environ. Health Perspect. 132, 36001.
Smiesko, M., 2013. DOLINA–docking based on a local induced-fit algorithm: application toward small-molecule binding to nuclear receptors. J. Chem. Inf. Model 53, 1415–1423.
Soderqvist, G., Poutanen, M., Wickman, M., von Schoultz, B., Skoog, L., Vihko, R., 1998. 17Beta-hydroxysteroid dehydrogenase type 1 in normal breast tissue during the menstrual cycle and hormonal contraception. J. Clin. Endocrinol. Metab. 83, 1190–1193.
Srnovrsnik, T., Virant-Klun, I., Pinter, B., 2023. Polycystic Ovary Syndrome and Endocrine Disruptors (Bisphenols, Parabens, and Triclosan)-A Systematic Review. Life (Basel) 13.
Stanojevic, M., Sollner Dolenc, M., 2025. Mechanisms of bisphenol A and its analogs as endocrine disruptors via nuclear receptors and related signaling pathways. Arch. Toxicol. 99, 2397–2417.
Thayer, K.A., Taylor, K.W., Garantziotis, S., Schurman, S.H., Kissling, G.E., Hunt, D., Herbert, B., Church, R., Jankowich, R., Churchwell, M.I., Scheri, R.C., Birnbaum, L. S., Bucher, J.R., 2016. Bisphenol A, Bisphenol S, and 4-Hydro xyphenyl 4-Isopro oxyphenyl sulfone (BPSIP) in Urine and Blood of Cashiers. Environ. Health Perspect. 124, 437–444.
Tsachaki, M., Odermatt, A., 2019. Subcellular localization and membrane topology of 17beta-hydroxysteroid dehydrogenases. Mol. Cell Endocrinol. 489, 98–106.
Tsachaki, M., Strauss, P., Dunkel, A., Navratilova, H., Mladenovic, N., Odermatt, A., 2020. Impact of 17beta-HSD12, the 3-ketoacyl-CoA reductase of long-chain fatty acid synthesis, on breast cancer cell proliferation and migration. Cell Mol. Life Sci. 77, 1153–1175.
Tsukamoto, S., Khavani, M., Domkam, N., Mofrad, M.R.K., 2024. Enhanced HP1α homodimer interaction force-induced salt bridge formation: implications for chromatin crosslinking and phase separation. Rsc Mechanochem 1, 78–93.
van den Brand, A.D., Hessel, E.V.S., Rijk, R., van de Ven, B., Leijten, N.M., Rorije, E., den Braver-Sewradj, S.P., 2024. A prioritization strategy for functional alternatives to bisphenol A in food contact materials. Crit. Rev. Toxicol. 54, 291–314.
van Leeuwen, S.P., Bovee, T.F., Awchi, M., Klijnstra, M.D., Hamers, A.R., Hoogenboom, R.L., Portier, L., Gerssen, A., 2019. BPA, BADGE and analogues: A new multi-analyte LC-ESI-MS/MS method for their determination and their in vitro (anti) estrogenic and (anti)androgenic properties. Chemosphere 221, 246–253.
Welshons, W.V., Nagel, S.C., vom Saal, F.S., 2006. Large effects from small exposures. III. Endocrine mechanisms mediating effects of bisphenol A at levels of human exposure. Endocrinology 147, S56–S69.
Wu, L., Einstein, M., Geissler, W.M., Chan, H.K., Elliston, K.O., Andersson, S., 1993. Expression cloning and characterization of human 17 beta-hydroxysteroid dehydrogenase type 2, a microsomal enzyme possessing 20 alpha-hydroxysteroid dehydrogenase activity. J. Biol. Chem. 268, 12964–12969.
Xu, X., Zhang, Y., Huang, H., Chen, J., Shi, T., 2024. Distribution, transformation, and toxic effects of the flame retardant tetrabromobisphenol S and its derivatives in the environment: A review. Sci. Total Environ. 948, 174799.

Ye, L., Zhao, B., Hu, G., Chu, Y., Ge, R.S., 2011. Inhibition of human and rat testicular steroidogenic enzyme activities by bisphenol A. Toxicol. Lett. 207, 137–142.
Zhao, N., Zhu, J., Zhao, M., Jin, H., 2023. Twenty bisphenol analogues in take-out polystyrene-made food containers: concentration levels, simulated migration, and risk evaluation. Environ. Sci. Pollut. Res Int 30, 10516–10526.
Zhao, Q., Howard, E.W., Parris, A.B., Ma, Z., Xing, Y., Yang, X., 2019. Bisphenol AF promotes estrogen receptor-positive breast cancer cell proliferation through amphiregulin-mediated crosstalk with receptor tyrosine kinase signaling. PLoS One 14, e0216469.